COOPERATIVE RESEARCH CENTRE FOR **CATCHMENT HYDROLOGY**

CLASS: CATCHMENT SCALE MULTIPLE-LANDUSE ATMOSPHERE SOIL WATER AND SOLUTE TRANSPORT MODEL

TECHNICAL REPORT
Report 04/12

December 2004

Narendra Kumar Tuteja / Jai Vaze / Brian Murphy / Geoffrey Beale

COOPERATIVE RESEARCH CENTRE FOR
CATCHMENT HYDROLOGY

Department of
Infrastructure, Planning and Natural Resources

Tuteja, Narendra Kumar.

CLASS: Catchment Scale Multiple-Landuse Atmosphere Soil Water and Solute Transport Model.

Bibliography

ISBN 1 920813 17 9

1. Hydrologic models. 2. Runoff - Mathematical models. I. Tuteja, Narendra Kumar. II. Cooperative Research Centre for Catchment Hydrology. III. Title. (Series : Report (Cooperative Research Centre for Catchment Hydrology); 04/12)

551.48011

Keywords

Land use
Catchment areas
Models
Soil water
Solutes
Transport
Water yield
Salinity
Salting
Geographic information systems
Water balance
Spatial distribution
Vegetation
Pastures
Hydrology
Recharge
Plant water relations

CLASS: Catchment Scale Multiple-Landuse Atmosphere Soil Water and Solute Transport Model

Narendra Kumar Tuteja / Jai Vaze / Brian Murphy / Geoffrey Beale

Department of Infrastructure, Planning and Natural Resources, New South Wales, Australia

Technical Report 04/12
December 2004

Preface

Since the beginning of computer based hydrological models in the 1960s and 1970s, there has been much debate regarding the appropriate structure and level of complexity of models. This reached fever pitch in the late 1980s and early 1990s as the cost of computing power reduced dramatically and a new generation of models provided information not only at catchment outlets, but also simulation of the spatial responses within the catchment. These are so called "process-based, distributed models" and the most complex of them are based on fundamental equations for the movement of water and solutes through porous media, hydraulic and hydrodynamic behaviour. They are characterised as "bottom-up" models where algorithms related to the myriad of processes that make up hydrological response are linked together, resulting in models with a very large number of parameters, many of which are "in principle" measurable but in practice can be difficult to define.

These models contrast with the "top-down" style of models that are conceptually simpler with fewer empirical parameters that are generally calibrated against observations, but are more limited in spatial detail and process representation. The modelling literature, particularly from the 1990s, includes many discussions on the philosophical, theoretical and practical advantages and disadvantages of the various approaches to modelling, with often quite polarised views.

In more recent times, there has been a wider acceptance of "horses for courses" – the need for a range of models of different complexity to meet the wide range of modelling applications and data availability. This technical report describes the modelling framework, CLASS, which is at the more complex end of the modelling spectrum, but where there has been a major effort made to exploit the ever-increasing range of available data for setting up and running the model. CLASS was developed by the New South Wales Department of Infrastructure, Planning and Natural Resources as an Associate Project of the Cooperative Research Centre (CRC) for Catchment Hydrology.

CLASS is a distributed, eco-hydrological modelling framework that deals with water and solute movement from hillslope to catchment scale. Considerable effort has been made in representing vegetation growth, as well as in the pathways that water takes from hillslope to stream. This capability enables detailed simulation of the effects of different management scenarios. CLASS includes user-friendly interfaces to assist the user in preparing the data needed for execution and testing. The science that underpins CLASS has been externally reviewed and is clearly described in this report.

Ultimately, CLASS will be incorporated into the Catchment Modelling Toolkit (www.toolkit.net.au) and will be one of a number of models of different complexity that represent water and solute movement. The CLASS modelling framework includes seven products that can be implemented at the hillslope scale. However, at the catchment scale CLASS is a computationally demanding modelling approach, and requires considerable skill to apply and interpret the model results, but is a powerful platform for detailed analysis and makes excellent use of the available data.

Rodger Grayson, Director
CRC for Catchment Hydrology

Acknowledgments

We wish to acknowledge the following for their contributions: John Gallant, Ian Johnson, Jim Morris, Jin Teng, Bill Johnston, David Tarboton, Yuri Ivailovski, Guy Geeves, Greg Summerell, Michelle Miller, Michael Williams and Sanmugan Prathapar. We thank Ross Williams, Dugald Black, Peter Barker and Charmaine Beckett for their support. New South Wales Government funded the work under the NSW Salinity Strategy. We thank Mark Wigmosta (Pacific Northwest National Lab., Richland, USA), Tomas Vogel (Czech Technical University, Prague, Czech Republic) and Rodger Grayson (CRC for Catchment Hydrology, Australia) for reviewing this work. This report has improved substantially from their review.

List of Figures

1. Introduction

Investigation of the vegetation effects in the atmosphere-soil-vegetation continuum on the catchment scale water balance has been a subject of extensive observation and modelling across the world for many years (Vertessy *et al.*, 1996). Complex distributed parameter process models such as SHE (Abbott *et al.*, 1986), TOPOG_IRM (Dawes and Hatton, 1993) and CATPRO (Ruprecht and Sivapalan, 1991) have been used to address these issues. While very useful, they require comprehensive calibration data sets to parameterise the many micro-scale processes incorporated in their procedures. As such they are used primarily as research tools rather than management tools. Process based one dimensional water balance models such as PERFECT (Littleboy *et al.*, 1992) and APSIM (McCown *et al.*, 1996), have been used in a GIS framework to investigate the effects of soils, landuse and land management practices on the near surface soil moisture dynamics and water balance components (eg. Ringrose-Voase and Cresswell, 2000). However, there is often a mismatch between the catchment scale fluxes and those obtained in a purely vertical analysis due to scale effects and no accounting of the lateral fluxes.

In recent times complex process modelling approaches have given way to more simplistic approaches due to issues of scale and data availability (Grayson and Blöschl, 2000). Many authors (eg. Holmes and Sinclair, 1986; Turner, 1991; Zhang *et al.*, 2001) have developed relationships between vegetation type and average annual evapotranspiration from a small number of readily available parameters. Although useful, these coarse average annual relationships provide insufficient information on the temporal effects of tributary flow required for water management purposes.

In upland areas with moderate to steep slopes, topography is an important variable that affects water balance and the magnitude of lateral fluxes in conjunction with the spatial distribution of soil types and landuse. Several topographic indices relating landscape position to surface and sub-surface runoff are commonly used (eg. Roberts *et al.*, 1997). The most commonly used index is called the wetness index (Beven and Kirkby, 1979) that under some circumstances (Grayson and Western, 2001) can be used to quantify runoff potential of different landscape elements. This index can be used to relate depth of the (perched) water table at any location in the catchment to mean depth of the (perched) water table over the catchment as in the TOPMODEL (Beven and Kirkby, 1979). The wetness index incorporates the effect of topography but does not account for the effects of soils and landuse. Therefore, a common situation encountered in catchment scale modelling is either inadequate accounting of the scale effects and lateral fluxes or inadequate accounting of the soil and vegetation effects.

A new generation of the distributed hydro-ecological models has been developed or is under development that attempt to simplify the complexity of applying a tightly bound theory and iterative numerical computations as in SHE and TOPOG. These models attempt to simplify excessive parameterisation and the numerical complexity associated with the distributed models. The structure of these models still retains the relevant internal processes of the climate-vegetation-soil-topography continuum and the relevant boundary conditions within the modelling paradigm. Examples of these models include various implementations of the TOPMODEL (Beven and Kirkby, 1979; Famiglietti *et al.*, 1992; Band *et al.*, 1993; Sivapalan *et al.*, 1997; Beven and Freer; 2001), HILLFLOW-3D (Bronstert, 1995), DHSVM (Wigmosta *et al.*, 1994), MACAQUE (Watson *et al.*, 1999; Watson *et al.*, 2001) and CATSALT (Tuteja *et al.*, 2003; Vaze *et al.*, 2004).

It is generally accepted that the spread of dryland salinity in the upper parts of the Murray-Darling Basin has resulted from the clearing of native vegetation for European-style agriculture (Walker *et al.*, 1992; Williamson *et al.*, 1997). A system of water quality targets, benchmarked at major basin outlets and strategic locations within each river basin network has been adopted (DLWC, 2000; MDBMC, 2001). These targets are intended to also facilitate the development of markets in salinity, carbon and biodiversity credits. A prerequisite for salinity management is modelling of the impacts of landuse change on water yields, salt export, and aquifer response times, to assess the biophysical capacity to change. CATSALT version 1.5 was developed to support assessment of the catchment

scale impacts of realistic and plausible landuse changes on stream flow and salinity (Vaze *et al.*, 2004; Tuteja *et al.*, 2003). It uses semi-distributed water and salt balance and a comprehensive framework for describing soil hydraulic properties and soil salinities.

CATSALT version 1.5 was developed as an intermediate product to support policy initiatives with regards to salinity. While the product has served its intended purpose and is better than most salinity modelling tools available in Australia, there are many limitations of version 1.5 that must be overcome, such as:

- CATSALT version 1.5 uses topographic wetness index as the basis for all computations. Many different landscape elements in the catchment can have the same wetness index. This produces difficulties in implementing landuse change scenarios.
- Averaging of salt concentration over the wetness index categories in the soil is unavoidable and this has implications for salt modelling.
- CATSALT version 1.5 apportions flow at the catchment outlet based on landuse and the wetness index or topography without explicit routing through the landscape. Effects of landuse change scenarios in a property can be seen at the catchment outlet and not at the properties at downstream landscape locations.
- CATSALT version 1.5 does not include vegetation growth and depends on other models (eg. PERFECT; Littleboy *et al.*, 1992).

A quantitative analysis of the impacts of climate and landuse change on water and salt yield from a catchment can be undertaken using a distributed hydrological model that can adequately represent system dynamics of the complex hydrological processes and operates on a pixel level. To overcome the above limitations, we have created a new distributed model, called the **C**atchment scale multiple-**l**anduse **a**tmosphere **s**oil water and **s**olute transport model (CLASS). The model is adapted to Australian conditions and is designed for accurate assessment of the paddock scale effects of landuse changes and climate variability on water and salt yield from the catchment. Our approach differs from earlier approaches in that the model is being designed to operate in data poor environments with the appropriate level of complexity. The distributed model DHSVM (Wigmosta *et al.*, 1994) is somewhat similar to our objectives and approach. Therefore where appropriate, parts of the water balance component of CLASS are adapted from DHSVM. This technical report describes key components of the CLASS model in detail including all the principal algorithms and the associated equations.

2. Overview of the CLASS Modelling Framework

The CLASS modelling framework consists of a suite of tools that can be used for physically based distributed eco-hydrological modelling (Figure 1). The framework is designed for investigation of the effects of landuse and climate variability on both paddock scale as well as the catchment scale. The framework includes the following tools that are used as building blocks in the catchment model.

CLASS Spatial Analyst - a fully automated GIS based tool required for spatial modelling (Teng *et al.*, 2004; released May 2004). It prepares all spatial information required by the catchment model. This includes: preparation of the climate surfaces and delineation of the climate zones, determination of the soil depth, water balance computational sequence using multiple flowpaths from terrain analysis and flow accumulation areas, wetness index, land discharge areas, soil salinity distribution and mapping of pixels to landuse and groundwater flow systems. A dynamic but constant user specified pixel size can be used depending on DEM resolution and size of the problem.

CLASS U3M-1D - a variable sub-daily time step model used for partitioning water balance in the unsaturated zone using the Richard's equation on a single pixel (Vaze *et al.*, 2004; released June 2004). Solutes are transferred between the soil materials using advection.

CLASS U3M-2D - a variable sub-daily time step model used for partitioning water balance in the unsaturated zone using the Richard's equation on a hillslope (Tuteja *et al.*, in prep. a). Solutes are transferred between the soil materials using advection.

CLASS PGM - a daily time step growth model based on Johnson (2003) that simulates up to five multiple pasture species that may be summer or winter active perennial/annual pasture and a legume (Vaze *et al.*, 2004a). Environmental conditions as well as soil water, nutrient and salinity status influences pasture growth and tissue dynamics.

CLASS CGM - a daily time step growth model based on Johnson (2003) that simulates a generic crop and its physiological structure and allows for complex interactions between light, temperature, available water and nutrients (Vaze *et al.*, 2004b).

CLASS 3PG+ - a monthly time step growth model that simulates tree growth using the 3-PG+ model (Morris, 2003), an adaptation of the 3PG model by Landsberg and Waring (1997) (Tuteja *et al.*, in prep. b).

CLASS Catchment Model - a distributed catchment scale model described in this report that operates on a pixel level and makes use of the above tools (Figure 2.2). Climate data and landuse information is used at each pixel for plant growth using CLASS PGM, CGM and 3PG+. Unsaturated zone water and solute balance is then performed using U3M-1D along the vertical axis. Excess moisture and the associated solutes are then estimated over each soil material. Water and solutes are transferred from up-slope properties to the down-slope properties and eventually to the catchment outlet using multiple flow paths and Darcian concepts. Additionally, spatial distribution of the soils, landuse, climate and groundwater flow system (GFS) links pixel scale dynamics to the catchment scale effects. Recharge and lateral throughflow each are pooled over the GFS. A proportion of each of these components is passed to the land as surface discharge and the remaining component is passed to the stream. Discharge to the land and stream is lagged appropriately and is based on the assumption that the bulk of the travel time results where the flow occurs under phreatic conditions, and that a fast pressure transmission signal applies under the confined conditions. Routing in the stream is based on the response function approach (Nash, 1960; Kachroo, 1992).

The model design accounts for data constraints often imposed in catchment scale investigations. Data requirements vary depending on the type of implementation ie. property scale or the catchment scale. The following primary data are required for implementation of the CLASS framework: climate data, DEM, Landuse, FLAG upness index, MRVBF index, GFS spatial distribution, hydraulic properties and solute concentration, soils spatial distribution, soil hydraulic properties, growth parameters, observed flow and solute concentration. Most of these data are

available on a wide spread basis. Sufficient tools and databases exist in the CLASS framework that allows for generating the information generally not available for catchment scale implementations (eg. soils, growth parameters and terrain analysis). All parameters required for the CLASS Catchment Model are described in the User's Manual (Tuteja *et al.*, in prep.c)

The CLASS modelling framework is supported by a user friendly graphical user interface. In 2004-05, the CLASS modelling framework will be incorporated into Toolkit Modelling Environment developed by the Cooperative Research Centre for Catchment Hydrology (Rahman *et al.*, 2003).

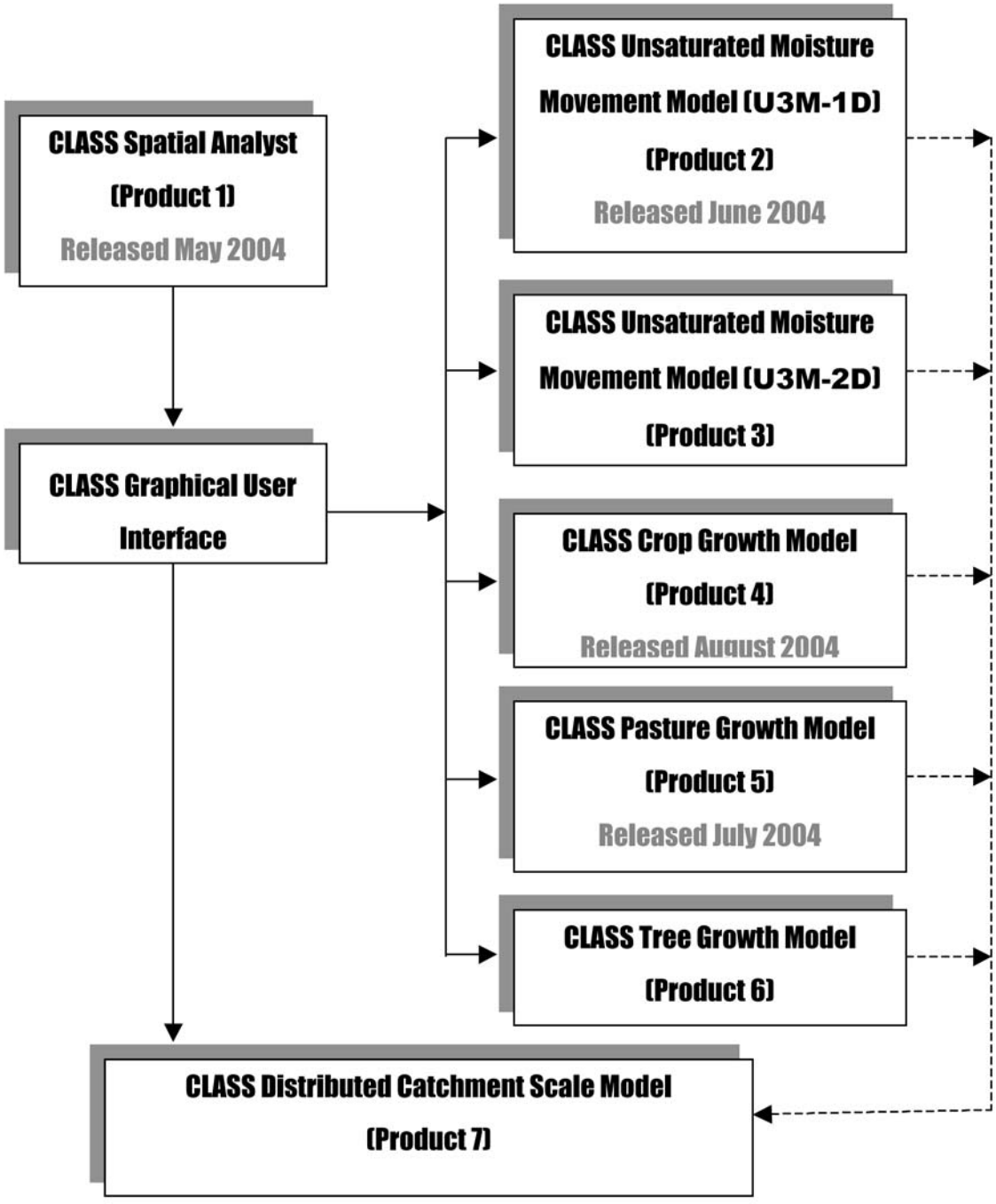

Figure 1. The CLASS Modelling Framework.

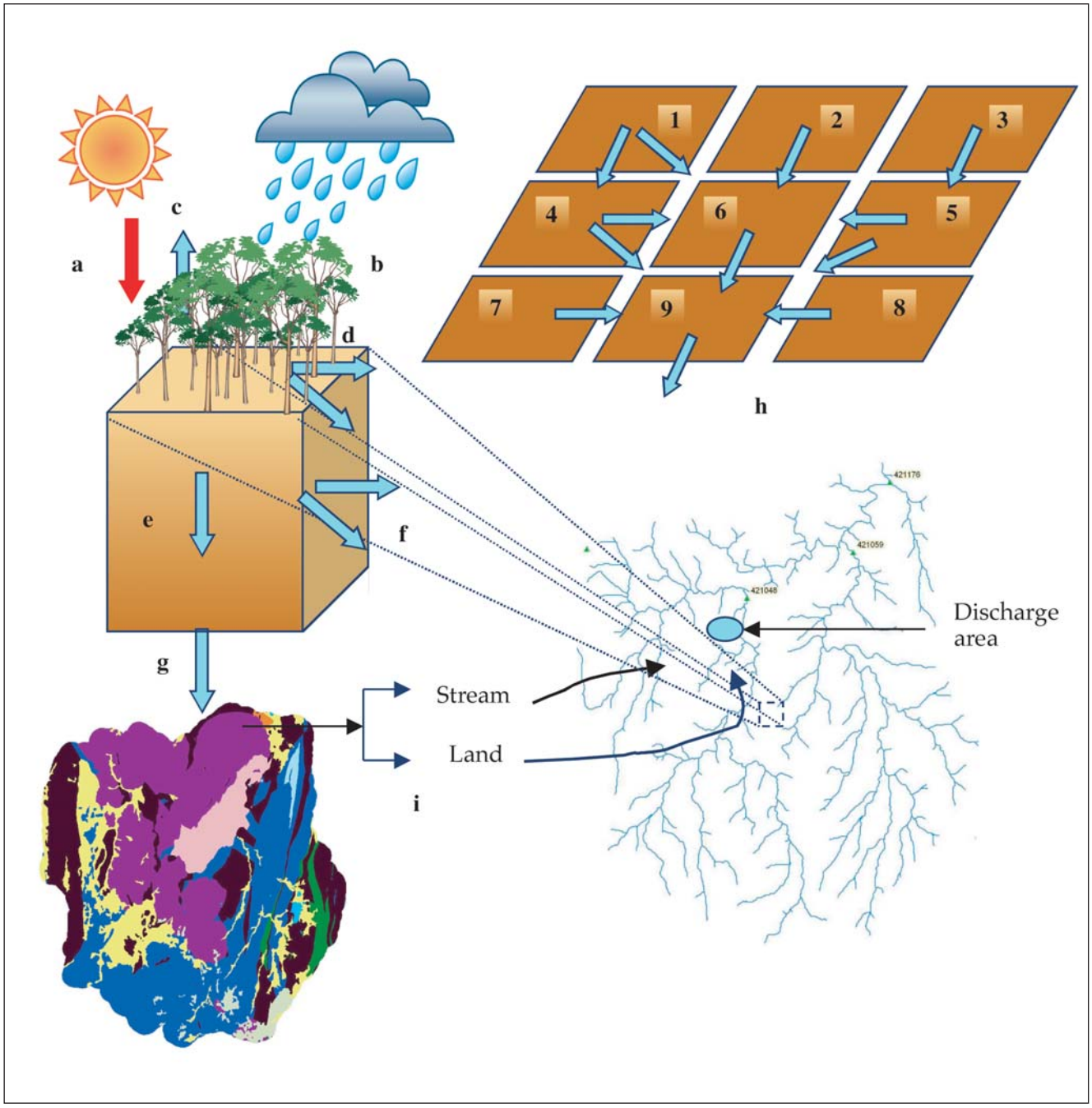

Figure 2. Schematic Diagram of Partitioning of the Water Balance Components and Simulated Landuse:- (a) solar radiation and climate data, (b) rainfall, (c) evapotranspiration, (d) overland flow, (e) flow through the soil, (f) shallow sub-surface flow, (g) drainage from the soil profile and recharge to the Groundwater Flow System (GFS), (h) water balance computational sequence (1-9), (i) discharge from groundwater to land and stream.

3. CLASS Water Balance and Plant Growth Components

3.1 Climate Data and Disaggregation of Daily Climate Data to Sub-daily Climate Data

Daily climate surfaces are available in Australia from the Silo database archived at Queensland Department of Natural Resources (Jeffrey *et al.*, 2001). Available climate data includes maximum and minimum air temperature, rainfall, pan evaporation, incoming short-wave radiation, vapour pressure, maximum and minimum humidity. Climate surfaces are available at 5 km grid for the whole of NSW and are used to describe climate forcing on the soil surface. In general four to six climate zones are formed and each pixel in the catchment is linked to a given climate zone to describe the atmospheric boundary condition.

Rainfall intensity relevant to the runoff generation must be reflected in the temporal resolution of the meteorological data and the modelling time step. Average rates over a time interval are invariably treated as constant rates within the time step in most models. If the time intervals are long (eg. 24 hours), the replacement of actual, highly variable instantaneous precipitation rates with daily averages may lead to an intolerably high underestimation of the overland flow and overestimation of the infiltration (Kandel *et al.*, 2002). Similar arguments pertain, to a lesser extent, to the soil evaporation rate, where the use of daily averages can lead to an unrealistic overdrying of the uppermost soil layer (Dolezal, 2002). It may be argued that the overall long-term hydrological behaviour of a soil profile can be satisfactorily modelled even if the fine diurnal dynamics is neglected.

In order to define the atmospheric boundary condition at the soil surface, an accurate estimate of the climate fluxes at a sub-daily time step is required. Disaggregation of the daily climate data into sub-daily climate data is adapted from Dolezal (2002). For rainfall disaggregation, an exponential distribution form is used and is adapted from the EPIC model (Sharpley *et al.*, 1990). Disaggregation of the potential evapotranspiration uses clear sky irradiance and is adapted from the work of a number of authors (eg. Beer, 1990; Burman and Pochop, 1994; Burman *et al.*, 1983; Monteith and Unsworth, 1990; Smith, 1991)

3.2 Topographic Modelling

3.2.1 Topographic Modelling for Estimation of the Spatial Distribution of Soils

Estimates of soil hydraulic properties across the landscape are a requirement for implementation of a distributed hydrologic model. Unfortunately there are few direct data on soil hydraulic properties at a catchment scale. Estimates of these properties have to be made using relationships based upon more routinely and more frequently collected soil property measurements. While a considerable amount has been written about the development of parametric Pedotransfer Functions (PTFs) to relate various soil physical, chemical and morphological properties to soil hydraulic properties, less has been written about how they can be applied to catchments. Spatial distribution of the individual soil types within individual soil landscapes is predicted using a DEM and terrain analysis and the framework of Murphy *et al.*, (2003).

Soil landscape units are frequently mapped and these are commonly topographic sequences of soils, with different soil types occupying different landform elements. The usual sequence consists of shallower, well-drained soils on crests and upper slopes, grading to deeper, poorly drained soils on lower slopes and depressions. Alluvial soils are associated with definable floodplains and terraces. The FLAG model (Roberts *et al.*, 1997) is used for terrain analysis to sub-divide the catchment into four slope classes (low, low to mid, mid to upper and upper slopes) to separate areas of individual soil types within soil landscapes (McDonald *et al.*, 1990; Summerell *et al.*, 2003a-b). The four slope classes are also referred to as the FLAG landforms. This enables prediction of the spatial distribution of individual soil types. The methodology makes the best possible use of the available soil information from soil maps, data bases, and secondary sources of information such as geology maps, geomorphology maps, and climate data. It is clear that this particular methodology assumes that the distribution of soil types within a soil landscape is defined by a toposequence. Where some other factors

control the distribution of soil types in a landscape, such as microclimate or short-range variation in parent materials, the methodology needs to be modified. A further complication occurs in using soil maps where a single toposequence is divided into two soil landscapes, as can occur with some more intensive mapping.

The identification of soils down to the soil type level enables the texture, structure and bulk density of the individual soil horizons to be predicted. The assumption is made that each Great Soil Group (Stace *et al.*, 1968) within a soil landscape is equivalent to a soil family or soil series. Relationships between texture and structure and soil hydraulic properties that have been developed in the literature and from other data sets are then used to predict the soil hydraulic properties of the individual soil types (see Section 3.3).

3.2.2 Topographic Modelling for Estimation of the Soil Depth and Soil Moisture Storage

Soils on the hillslopes are generally shallow and the landscape processes are characterised by erosion while deeper soils in deposition environment occur on the valley bottoms. Distinguishing valley bottoms from hillslopes is important to determine soil depths and soil moisture holding capacities across the landscape. Gallant and Dowling (2003) have presented a new index, called the Multi-Resolution Valley Bottom Flatness index (MRVBF) for delineating depositional areas from the erosion areas high in the landscape. Their methodology operates at a range of scales and combines the results at different scales into a single index that can be related to predict soil depth and soil moisture storage capacity.

McKenzie *et al.*, (2003) presented a methodology to predict soil depth and soil moisture storage capacity for medium sized catchments. They predicted soil depth based on the wetness index and MRVBF in the erosional and depositional landscapes respectively. A smooth weighting function was introduced that gave more weightage to wetness index at locations high in landscape. The weighting for wetness index decreases gradually while MRVBF weighting increases at locations low in the landscape. This framework is used in CLASS along with spatial distribution of the soils to predict soil depth and soil moisture storage capacity.

3.2.3 Topographic Modelling for Determining Hydrological Flow Paths and the Upstream Contributing Areas

Many schemes are available for calculating hydrological flowpaths and the upstream contributing area at any given location in the catchment (eg. O'Callaghan and Mark, 1984; Quinn *et al.*, 1991; Lea, 1992; Costa-Cabral and Burges, 1994; Tarboton, 1997). Tarboton (1997) proposed a new multiple flow path algorithm, called the D∞ method, that performed better than most other methods.

This method is used in CLASS for estimating hydrological flowpaths and is used for horizontal distribution of the saturated sub-surface flow by advection. The method is based on representing resultant flow direction as a single angle taken as the steepest downward slope on the eight triangular facets centred at each grid point. Flow is then apportioned to the two-downslope pixels on the basis of angle between the resultant flow direction and the angles of the downslope pixels.

3.3 Soil Pedotransfer Function (PTF) Models for Parameterisation of the Soil Hydraulic Properties

Spatial distribution of soils in the catchment and their physical properties (eg. texture, structure, soil horizons and bulk density etc.) are determined using the methodology of Murphy *et al.*, (2003) (Section 3.2.1). Parametric PTFs can then be used to estimate soil hydraulic parameters describing variation of pressure head with soil moisture and unsaturated hydraulic conductivity (eg. Wösten *et al.*, 1995; Schaap *et al.*, 1998; Minasny and McBratney, 2002). Minasny and McBratney (2002) proposed a new method called the neuro-m method, wherein parameter estimation by the artificial neural network is matched against the measured data. Using Australian data as a training set these authors demonstrated substantial improvement in accuracy of the PTFs obtained from neuro-m method compared to those obtained from published neural network based PTFs. This method is used for estimating soil hydraulic parameters of the van Genuchten's soil hydraulic model (van Genuchten, 1980). Two additional soil hydraulic models by Vogel and Cislerova (1988) and Brooks and Corey (1966) are also available in CLASS

U3M. Preset soil parameters based on the soil type are also built into the model from published databases (Carsel and Parrish, 1988; van Genuchten *et al.*, 1991).

3.4 Multiple Landuse and Radiation Balance Model

The overstory shortwave radiation balance accounts for canopy reflectance, ground cover, radiation attenuation and is given by Equation 3.4.1.

$$R_{so} = R_s\left((1-\alpha_0)\downarrow - \exp(-k\,LAI_o)(1-\alpha_o)\downarrow\right)F_o \tag{3.4.1}$$

where:

R_{so} = shortwave radiation absorbed by the overstory (Wm^{-2}),

R_s = incident shortwave radiation (Wm^{-2}),

α_0 = overstory albedo (-),

k = canopy attenuation coefficient (-),

LAI_o = overstory LAI,

F_o = overstory groundcover fraction (-).

The understory receives attenuated shortwave radiation from the overstory and direct shortwave radiation where there is no overstory (see Equation 3.4.2).

where:

R_{su} = shortwave radiation absorbed by the understory (Wm^{-2}),

α_u = understory albedo (-),

LAI_u = understory LAI.

Shortwave radiation absorbed by the soil surface includes attenuated radiation from the understory and is given by Equation 3.4.3.

where:

R_{sg} = shortwave radiation absorbed by the soil surface (Wm^{-2}),

α_g = ground surface albedo (-).

The overstory longwave radiation balance is given by Equation 3.4.4.

where:

R_{lo} = absorbed overstory longwave radiation (Wm^{-2}),

L_d = $\varepsilon_a\sigma(T_a+273)^4$
= downward longwave radiation (Wm^{-2}),

T_a = air temperature above the canopy (^oC),

ε_a = $0.7+5.95\times10^{-5}e_a\exp(1500/(T_a+273))$
= clear sky atmospheric emissivity (-) (Idso, 1981),

T_o = overstory temperature (assumed same as the air temperature ^oC),

e_a = vapour pressure (mb),

T_u = understory temperature (assumed same as the air temperature ^oC),

σ = Stefan-Boltzmann constant ($Wm^{-2}K^{-4}$).

$$R_{su} = R_s F_o(1-\alpha_o)\exp(-k\,LAI_o)(1-\alpha_u)\left(1-\exp(-kLAI_u)\right) + R_s(1-F_o)(1-\alpha_u)\left(1-\exp(-kLAI_u)\right) \tag{3.4.2}$$

$$R_{sg} = R_s F_o(1-\alpha_o)\exp(-k\,LAI_o)(1-\alpha_u)\exp(-k\,LAI_u)(1-\alpha_g) + R_s(1-F_o)(1-\alpha_u)\exp(-kLAI_u)(1-\alpha_g) \tag{3.4.3}$$

$$R_{lo} = \left(L_d\downarrow + \sigma(T_u+273)^4\uparrow - 2\sigma(T_o+273)^4\downarrow\uparrow\right)F_o \tag{3.4.4}$$

$$R_{lu} = \left(\sigma(T_o+273)^4\downarrow + \sigma(T_g+273)^4\uparrow - 2\sigma(T_u+273)^4\downarrow\uparrow\right)F_o + \left(L_d\downarrow + \sigma(T_g+273)^4\downarrow - 2\sigma(T_u+273)^4\downarrow\uparrow\right)(1-F_o) \tag{3.4.5}$$

The understory longwave radiation balance with the overstory and ground is given by Equation 3.4.5.

where:

R_{lu} = absorbed understory longwave radiation (Wm^{-2}),

T_g = soil surface temperature (assumed same as the air temperature ºC).

Longwave radiation balance of the ground surface is given by Equation 3.4.6.

where:

R_{lu} = absorbed understory longwave radiation (Wm^{-2}).

The climate variables R_s,R_{sj},T_j,T_g *and* L_d vary in time (d) and are averaged over the climate zone (j refers to either the overstory or the understory). The landuse variables LAI_j and F_j vary in time (d) and space (pixel) and are obtained from the growth models (Sections 3.8, 3.9 and 3.10).

3.5 Interception Model

The interception storage capacity for a canopy j for a given time step ($t+\delta t$) is estimated from LAI at the end of previous time step (t) (Dickinson, 1991; Wigmosta *et al.*, 1994).

$$I_{cj}(t+\delta t) = 10^{-4} LAI_j(t) F_j(t) \qquad (3.5.1)$$

where:

I_{cj} = Interception storage capacity of the canopy with j representing either the overstory I_{co} or the understory I_{cu} (m),

F_j = ground cover fraction of the canopy j.

Under growth limiting conditions imposed mainly by vapour pressure deficits, LAI for the overstory generally reaches a maximum of 4 (Landsberg and Waring, 1997). Assuming ground cover fraction to be one, maximum interception storage capacity of 0.4 mm is obtained for the overstory. This is similar to the interception storage capacity of 0.35 mm for the evergreen forest canopy obtained from experimental observations by Dunin *et al.*,(1988). For pasture and cropping, interception storage capacity would vary between 0 and 0.4 mm.

Denoting interception storage as $S_{ij}(m)$, potential evaporation ($E_{pj}m.s^{-1}$) from the wet canopy ($S_{ij}>0$) is obtained as in Equation 3.5.2.

where:

R_{nj} = net absorbed radiation ie. sum of canopy shortwave and longwave radiation ($W.m^{-2}$),

ρ = density of the moist air ($kg.m^{-3}$),

C_p = specific heat of the air ($J.kg^{-1}.K^{-1}$),

e_a,e_s = vapour pressure and saturated vapour pressure respectively at a given air temperature (mb) (Equation 3.5.10),

r_{aj} = aerodynamic resistance of the canopy $j(s.m^{-1})$,

γ = psychrometric constant ($mb.K^{-1}$),

Δ = slope of the saturated vapour pressure-temperature curve ($mb.K^{-1}$) (Equation 3.5.11),

λ = latent heat of vaporisation ($J.kg^{-1}$),

ρ_w = density of water ($kg.m^{-3}$).

$$R_{lg} = \left(\sigma(T_u + 273)^4 \downarrow - \sigma(T_g + 273)^4 \uparrow\right) \qquad (3.4.6)$$

$$E_{pj}(t+\delta t) = \frac{1}{\rho_w} \frac{\Delta R_{nj}(t+\delta t) + \rho C_p \dfrac{e_s(t+\delta t) - e_a(t+\delta t)}{r_{aj}(t+\delta t)}}{\lambda(\Delta+\gamma)} \qquad (3.5.2)$$

$$E_{ij}(t+\delta t) = \min\left(E_{pj}(t+\delta t), S_{ij}(t)/\delta t\right) \qquad (3.5.3)$$

Computation procedure for the aerodynamic resistance is described in Section 3.7.1. Actual evaporation from the canopy interception storage (E_{ij} $m.s^{-1}$) is constrained as minimum of moisture available in interception storage and the potential evaporation (see Equation 3.5.3).

Actual interception storage of the overstory is calculated as in Equation 3.5.4.

where:

P = precipitation rate ($m.s^{-1}$).

When water in the overstory interception storage ($S_{io}(t+\delta t)$) is in excess of the transient overstory interception storage capacity $I_{co}(t+\delta t)$, overstory throughfall and interception storage are adjusted as in Equations 3.5.5 and 3.5.6.

where:

$P_o(t + \delta t)$ = overstory throughfall rate ($m.s^{-1}$).

Actual interception storage of the understory is calculated as in Equation 3.5.7.

where:

P_O = overstory throughfall rate ($m.s^{-1}$).

When water in the understory interception storage ($S_{iu}(t+\delta t)$) is in excess of the transient interception storage capacity $I_{co}(t+\delta t)$, understory throughfall and interception storage are adjusted as in Equations 3.5.8 and 3.5.9.

where:

$P_u(t + \delta t)$ = understory throughfall rate ($m.s^{-1}$).

$$S_{io}(t+\delta t) = \max\left[0, S_{io}(t) + \left(P(t+\delta t) - E_{io}(t+\delta t)\right)\delta t\right] \tag{3.5.4}$$

$$P_o(t+\delta t) = \begin{cases} \left(S_{io}(t+\delta t) - I_{co}(t+\delta t)\right)/\delta t & \text{if } S_{io}(t+\delta t) > I_{co}(t+\delta t) \\ 0 & \text{if } S_{io}(t+\delta t) \le I_{co}(t+\delta t) \end{cases} \tag{3.5.5}$$

$$S_{io}(t+\delta t) = I_{co}(t+\delta t) \quad \text{if } S_{io}(t+\delta t) > I_{co}(t+\delta t) \tag{3.5.6}$$

$$S_{iu}(t+\delta t) = \max\left[0, S_{iu}(t) + \left(P_o(t+\delta t) - E_{iu}(t+\delta t)\right)\delta t\right] \tag{3.5.7}$$

$$P_u(t+\delta t) = \begin{cases} \left(S_{iu}(t+\delta t) - I_{cu}(t+\delta t)\right)/\delta t & \text{if } S_{iu}(t+\delta t) > I_{cu}(t+\delta t) \\ 0 & \text{if } S_{iu}(t+\delta t) \le I_{cu}(t+\delta t) \end{cases} \tag{3.5.8}$$

$$S_{iu}(t+\delta t) = I_{cu}(t+\delta t) \quad \text{if } S_{iu}(t+\delta t) > I_{cu}(t+\delta t) \tag{3.5.9}$$

Saturated vapour pressure and its slope as a function of temperature in Equation 3.5.2 are obtained from Equation 3.5.10 and Equation 3.5.11 respectively (Equation 521, p172/2, Dolezal, 1994).

$$e_s(T) = \frac{A_e}{100}\exp\left(\frac{B_e T}{T + C_e}\right) \qquad (3.5.10)$$

$$\Delta = \frac{A_e B_e C_e}{100(T + C_e)^2}\exp\left(\frac{B_e T}{T + C_e}\right) \qquad (3.5.11)$$

where:

e_s = saturated vapour pressure (*mb*),

T = air temperature (°*C*),

Δ = slope of the vapour pressure temperature curve (*mb*.°K^{-1} or *mb*.°C^{-1}),

A_e = 610.78 (constant),

B_e = 17.269 (constant),

C_e = 237.3 (constant).

3.6 Infiltration Model

Infiltration rate is estimated using Yu's approach (Yu, 1997).

$$I_{cap} = I_p\left(1 - \exp\left(-\frac{P_u}{I_p}\right)\right) \qquad (3.6.1)$$

$$I_p = I_0\left(\frac{S}{S_{\max}}\right)^{-a} \qquad (3.6.2)$$

where:

I_{cap} = actual infiltration rate/capacity ($m.s^{-1}$),

P_u = Understory throughfall rate or net precipitation after accounting for canopy interception ($m.s^{-1}$),

I_p = spatially averaged potential infiltration rate ($m.s^{-1}$),

S = soil storage (*m*),

S_{max} = soil storage capacity (*m*),

I_0 = spatially averaged limiting infiltration rate, when saturation occurs over the entire pixel that generates runoff ($m.s^{-1}$),

a = parameter that depends on soil texture, slope steepness and soil surface conditions (basically a dimensionless calibration parameter).

The limiting infiltration rate I_0 can be considered as the effective saturated hydraulic conductivity at the soil surface, which may quantitatively differ from the subsurface hydraulic conductivity for physical and biological reasons. Kandel *et al.*,(2002) reported that the calibration parameter "a" in Equation 3.6.3 is highly variable (0.2 – 5.0). Analysis of Equation 3.6.2 for a range of S_{max}, I_0 and a values indicated that Equation 3.6.2 can be replaced by an alternative form described by Equation 3.6.3. For a given value of S_{max} and I_0, variation of $I_p(S)$ with S from Equation 3.6.3 is similar to that from Equation 3.6.2 for average range of a between 2 and 3. The advantage of Equation 3.6.3 is that the sensitive calibration parameter "a" is not required as in Equation 3.6.2 and the effects of changing sorptivity with moisture content and storage are accounted for.

$$I_p = I_0\exp\left(\frac{S_{\max} - S}{S_{\max}}\right) \qquad (3.6.3)$$

3.7 Evapotranspiration Sub-model

The evapotranspiration module is adapted from Wigmosta *et al.*,(1994), Shuttleworth and Wallace (1985), Dickinson *et al.*,(1991), Monteith (1973) and Monteith (1981). Actual transpiration from the dry canopy is estimated using Penman Monteith formulation (Monteith, 1981) (See Equation 3.7.1 below).

$$E_{tj}(t + \delta t) = \frac{1}{\rho_w}\frac{\Delta R_{nj}(t + \delta t) + \rho C_p\dfrac{e_s(t + \delta t) - e_a(t + \delta t)}{r_{aj}(t + \delta t)}}{\lambda\left(\Delta + \gamma\dfrac{r_{aj} + r_{sj}^c}{r_{aj}}\right)} \qquad (3.7.1)$$

where:

E_{tj} = actual plant transpiration ($m.s^{-1}$),

r_{aj} = aerodynamic resistance ($s.m^{-1}$),

r_{sj}^{c} = bulk stomatal resistance of the canopy ($s.m^{-1}$).

3.7.1 Aerodynamic and Canopy Resistance

The aerodynamic resistance r_{aj} in Equation 3.7.1 is calculated using energy combination theory (Figure 3) and a three layered distribution model of Shuttleworth and Wallace (1985) (Figure 4) as in Wigmosta *et al.*,(1994). The resistances shown in Figure 3 describe partitioning of the sensible and latent heat fluxes from different canopy and ground components.

Sufficient aerodynamic mixing is assumed to occur within the understory and the overstory such that the concept of mean understory and overstory canopy airstream is valid (Thom, 1972). Bulk boundary layer resistance ($r_{aj}^{c}\ s.m^{-1}$) controls transfer (water vapour and heat) between surface of the vegetation and the respective mean canopy airstream. For a fully developed canopy this resistance is often small (~ $3s.m^{-1}$ for LAI of about 4). Bulk stomatal resistance for the vegetation ($r_{sj}^{c}\ s.m^{-1}$) controls vapour flux from plant leaves to the boundary layer. The resistance at the soil surface ($r_{s}^{s}\ s.m^{-1}$) describes evaporation from wet soil below a dry soil layer of increasing thickness, treated as isothermal (Monteith, 1981).

Three aerodynamic resistances control vertical transport of the heat fluxes (Figures 3 and 4). The first resistance (r_{ao}^{a} or $r_{\log}^{I}\ s.m^{-1}$) controls vertical transfer between mean overstory airstream and the reference height Y. A logarithmic distribution is used above the canopy for the eddy diffusion resistance (Zone I; Figure 4). The second resistance (r_{au}^{a} or $r_{\exp}\ s.m^{-1}$) controls vertical transfer between mean understory airstream and the mean overstory airstream. Between the overstory and the understory an exponential distribution form of the eddy diffusion resistance is used r_{exp} (Zone II; Figure 4). The third resistance (r_{ag}^{a} or $r_{\log}^{III}\ s.m^{-1}$) controls vertical transfer from the soil surface before being incorporated into the mean understory airstream. A logarithmic distribution is used above the soil surface for the eddy diffusion resistance (Zone III; Figure 4).

Aerodynamic resistances across the three zones are considered in series when used in Penman Monteith equation as in Equations 3.7.2 and 3.7.3.

$$r_{ao} = r_{ao}^{c} + r_{ao}^{a} = r_{ao}^{c} + r_{\log}^{I} \qquad (3.7.2)$$

$$r_{au} = r_{au}^{c} + r_{au}^{a1} + r_{ao}^{a} = r_{au}^{c} + r_{\exp}^{1} + r_{\log}^{I} \qquad (3.7.3)$$

$$r_{ag} = r_{ag}^{a} + r_{au}^{a2} + r_{ao}^{a} = r_{\log}^{III} + r_{\exp}^{2} + r_{\log}^{I} \qquad (3.7.4)$$

where:

r_{au}, r_{ao}, r_{ag} are the resistances across the understory, overstory and near the soil surface respectively ($s.m^{-1}$).

Mean stomatal resistance and the vegetation density influence the bulk stomatal resistance r_{sj}^{c} of the canopy j as in Equation 3.7.5.

$$r_{sj}^{c} = \frac{r_{ST}}{2LAI_{j}\,GLF} \qquad (3.7.5)$$

where:

r_{ST} = mean stomatal resistance (~ 400 $s.m^{-1}$),

LAI_{j} = Leaf area index of the canopy j (varying in time and space and is obtained from the growth models) ($m^{2}.m^{-2}$),

GLF = growth limiting factor expressed as a product of water, nutrient and salinity stresses and is obtained from the growth module (Equation 2.14b, p21, Johnson, 2003).

Water and salinity stresses included in *GLF* vary in time and space while nutrient stresses are based on knowledge of the soil nutrient status. In the current version of the model, explicit nutrient modelling is not included.

Bulk boundary layer resistance (r_{aj}^{c}) of the canopy j depends on the mean boundary layer resistance and the vegetation density as in Equation 3.7.6.

$$r_{aj}^{c} = \frac{r_{bj}}{2LAI_{j}} \qquad (3.7.6)$$

where:

r_{bj} = mean boundary layer resistance (~ 25 $s.m^{-1}$).

The surface resistance of the soil r_s^s equals zero for the wet soil and is about 2000 $s.m^{-1}$ for dry sandy soils (Fuchs and Tanner, 1967). For soils of different texture and bulk density, it varies in a wide range.

The total available energy is the sum of latent and sensible heat flux (Equation 3.7.7) and the respective component heat fluxes can be added to get the total latent heat and total sensible heat fluxes (Equations 3.7.8 to 3.7.9).

$$A = \lambda E \rho_w + H \tag{3.7.7}$$

$$\lambda E \rho_w = \lambda E_s \rho_w + \lambda E_{tu} \rho_w + \lambda E_{to} \rho_w \tag{3.7.8}$$

$$H = H_s + H_{tu} + H_{to} \tag{3.7.9}$$

where:

A = total available energy ($W.m^{-2}$),

$\lambda E \rho_w$ = total latent heat flux ($W.m^{-2}$),

$\lambda E_s \rho_w$ = latent heat flux from soil evaporation ($W.m^{-2}$),

$\lambda E_{tj} \rho_w$ = latent heat flux from the canopy j ($W.m^{-2}$),

H = total sensible heat flux ($W.m^{-2}$),

H_s = sensible heat flux from soil evaporation ($W.m^{-2}$),

H_{tj} = sensible heat flux from the canopy j ($W.m^{-2}$).

Using the above canopy terms in an energy balance for sparse canopy, Shuttleworth and Wallace (1985) obtained a combination equation for evaporation from partial canopy. The equation correctly defines the asymptotic limits of evaporation from bare soil or complete canopy and collapses to the Penman Monteith equation (Equation 3.7.1).

3.7.1.1 Aerodynamic Resistance under a Fully Developed Canopy

Aerodynamic resistance between the overstory and the overlying boundary layer is given by Equation 3.7.10.

$$r_{ao}^a = r_{\log}^l = \frac{\left(\ln\left(\frac{Y_o - d_o}{z_{0o}}\right)\right)^2}{u(Y)k^2} \tag{3.7.10}$$

where:

Y_o = $h_o + Y$ (m),

Y = reference height (m),

d_o = overstory zero plane displacement (equal to $0.63h_o$) (m),

u = wind speed at reference height Y ($m.s^{-1}$),

k = von Karman constant (0.41),

h_o = overstory height (m),

Z_{0o} = overstory roughness length (equal to $0.13h_o$) (m).

Aerodynamic resistance for momentum transfer between the overstory and the understory are obtained using the exponential profile and is given by Equations 3.7.11 and 3.7.12. Equation 3.7.11 describes resistance to vertical eddy diffusion between $d_u + z_{0u}$ and $d_o + z_{0o}$ and is used when calculating r_{au}^{a1} in Equation 3.7.3. Equation 3.7.12 describes resistance to vertical eddy diffusion between z_n and $d_o + z_{0o}$ and is used when calculating r_{au}^{a2} in Equation 3.7.4.

$$r_{au}^{a1} = r_{\exp}^1 = \int_{d_u + z_{0u}}^{d_0 + z_{0o}} \frac{dz}{K_e} \tag{3.7.11}$$

$$r_{au}^{a2} = r_{\exp}^2 = \int_{z_n}^{d_0 + z_{0o}} \frac{dz}{K_e} \tag{3.7.12}$$

where:

K_e = eddy diffusion coefficient between the overstory and the understory (equals logarithmic diffusion coefficient K_l at the top of the overstory) ($m^2.s^{-1}$),

h_u = understory height (m),

d_u = understory zero plane displacement (equal to $0.63h_u$) (m),

z_{ou} = understory roughness length (equal to $0.13h_u$),

z_n = $0.1h_u$.

The eddy diffusion coefficient K_e is estimated using Equations 3.7.13 and 3.7.14.

$$K_e = K_l(h_0)\exp\left[n'\left(\frac{z}{h_0} - 1\right)\right] \tag{3.7.13}$$

$$K_l(h_0) = \frac{u(Y)k^2(h_0 - d_0)}{\ln\left(\frac{Y - d_0}{z_{0o}}\right)} \qquad (3.7.14)$$

where:

K_l = logarithmic diffusion coefficient ($m^2.s^{-1}$),

n' = extinction coefficient between 2 and 3 (dimensionless).

Substituting Equations 3.7.13 and 3.7.14 into Equations 3.7.11 and 3.7.12, the aerodynamic resistances $r^1_{\exp}$ and $r^2_{\exp}$ are obtained (see Equations 3.7.15 and 3.7.16 below).

where:

Z_{0u} = is the roughness length of the understory (equal to $0.13h_u$) (*m*),

Z_n = $0.1h_u$.

$$r^{a1}_{au} = r^1_{\exp} = \frac{h_0 e^{n'}}{n' K_l(h_0)}\left[\exp\left(\frac{-n'(d_u + z_{0u})}{h_0}\right) - \exp\left(\frac{-n'(d_0 + z_{0o})}{h_0}\right)\right] \qquad (3.7.15)$$

$$r^{a2}_{au} = r^2_{\exp} = \frac{h_0 e^{n'}}{n' K_l(h_0)}\left[\exp\left(\frac{-n' z_n}{h_0}\right) - \exp\left(\frac{-n'(d_0 + z_{0o})}{h_0}\right)\right] \qquad (3.7.16)$$

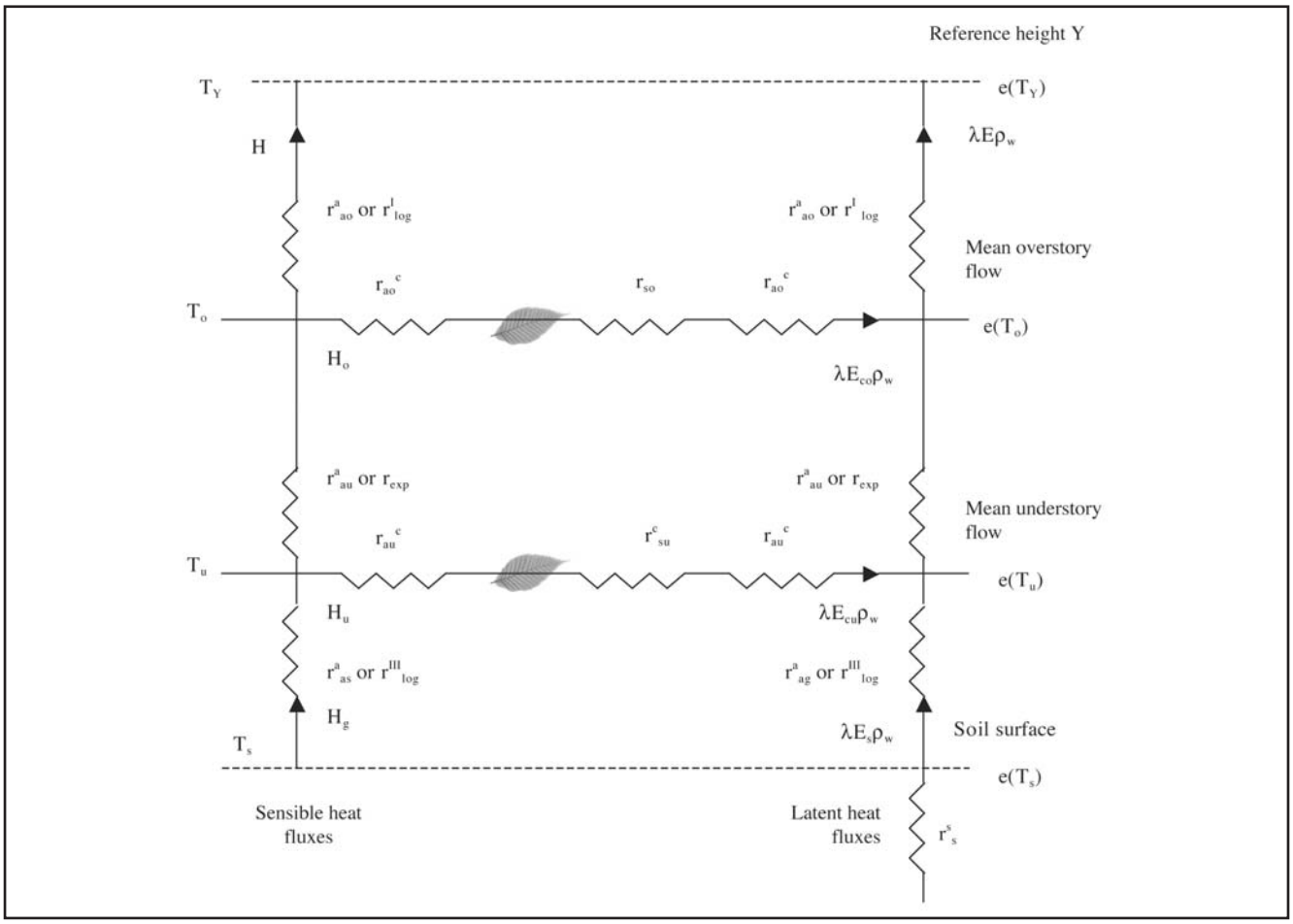

Figure 3. Schematic Diagram of the Energy Distribution for Partial Canopy.
(adapted from Shuttleworth and Wallace, 1985 and Wigmosta *et al.*, 1994). Total latent heat flux ($\lambda E\rho_w$; $W.m^{-2}$) and total sensible heat flux (H; $W.m^{-2}$) are sum of the respective individual heat components. Resistances ($s.m^{-1}$) to the individual energy flux are denoted by the following:- horizontal bulk boundary layer resistance (r^c_{aj}), bulk stomatal resistance of the canopy (r^c_{sj}), soil surface resistance (r^s_s), vertical aerodynamic resistance (r^a_a). T_j and T_s denote temperature of the canopy and the soil surface respectively.

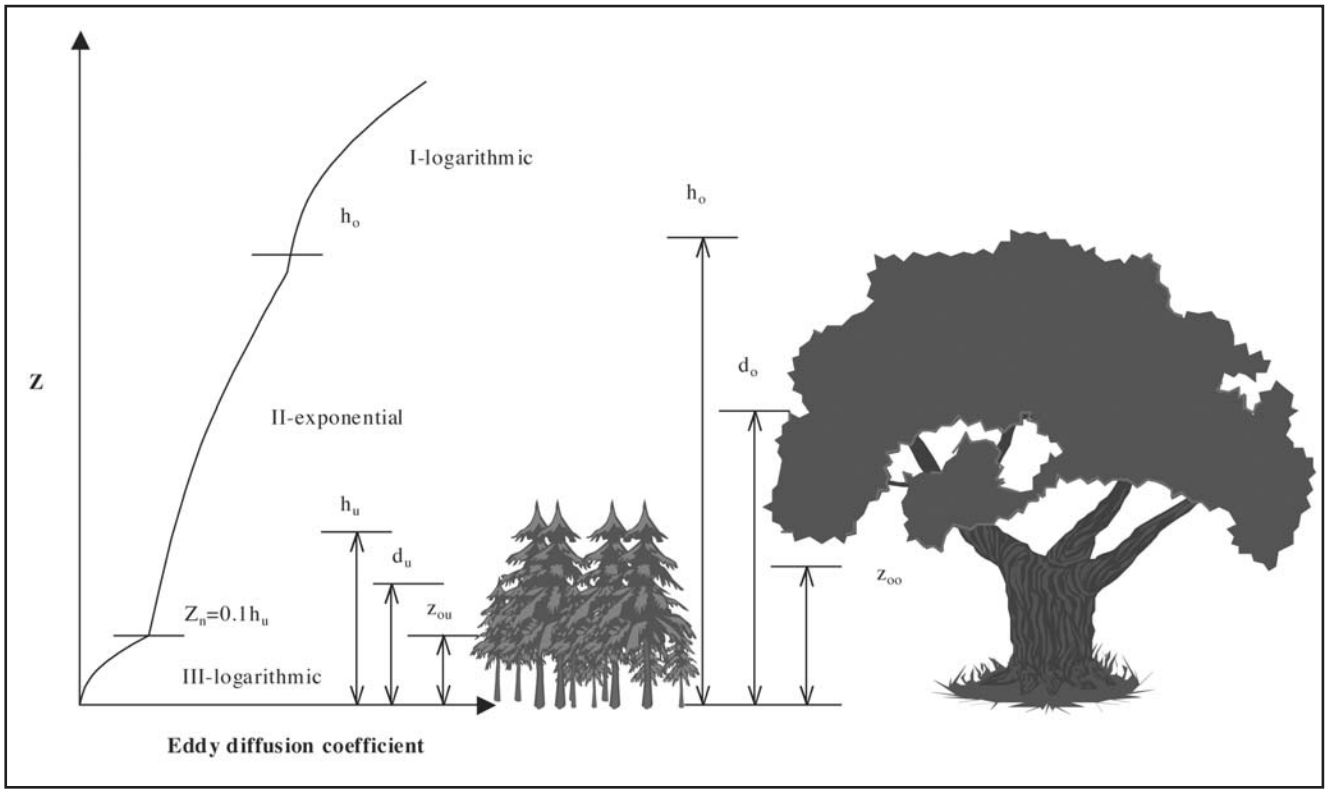

Figure 4. Three Layered Distribution for Estimation of the Aerodynamic Resistance (adapted from Shuttleworth and Wallace, 1985 and Wigmosta *et al.*,1994)

Aerodynamic resistance between the soil surface and the understory is given by Equation 3.7.17.

$$r_{ag}^{a} = r_{\log}^{III} = \frac{\left(\ln\left(\frac{z_n}{z_{0g}}\right)\right)^2}{u(z_n)k^2} \qquad (3.7.17)$$

where:

z_n = $0.1h_u$ and z_{0g} is the roughness length of the ground (m). The roughness length of the ground surface is commonly taken as 0.01 m (van Bavel and Hillel, 1976),

$u(z) = u(Y)(z/h_u)^{\alpha_{zn}}$, $0 \le \alpha \le 1$.

.

3.7.1.2 Aerodynamic Resistance with No Overstory

In the case of no overstory, the exponential distribution (Zone II, Figure 4) extends from z_n (~$0.1h_u$) to the mean understory flow height (~0.76 h_u) and thereafter a logarithmic distribution is assumed. Aerodynamic resistances across the three zones are again considered in series to estimate r_{au} and r_{ag}.

$$r_{au} = r_{au}^{c} + r_{au}^{a1} \qquad (3.7.18)$$

$$r_{ag} = r_{au}^{a1} + r_{\exp} + r_{ag}^{a} = r_{au}^{a1} + r_{\exp} + r_{\log}^{III} \qquad (3.7.19)$$

$$r_{au}^{a1} = \frac{\left(\ln\left(\frac{Y_u - d_u}{z_{0u}}\right)\right)^2}{u(Y)k^2} \qquad (3.7.20)$$

where:

$r_{\log}^{III}$ is estimated from Equation 3.7.17,

Y_u = $h_u + Y(m)$.

$$r_{\exp} = \frac{\ln\left(\frac{Y_u - d_u}{z_{0u}}\right)}{u(Y)k^2} \frac{h_u e^{n'}}{(h_u - d_u)n'} \left[\exp\left(\frac{-n'z_n}{h_u}\right) - \exp\left(\frac{-n'(d_u + z_{0u})}{h_u}\right)\right] \qquad (3.7.21)$$

3.7.1.3 Aerodynamic resistance with Partial Overstory

The aerodynamic resistance is assumed to vary linearly with the product of overstory LAI and ground cover (F_o) between the limits of fully developed overstory and no overstory. The aerodynamic resistances r_{aj} are first calculated for the fully developed overstory (Section 3.7.1.1) and then for the case of no overstory (Section 3.7.1.2). A linear interpolation is then performed as shown below in Equation 3.7.22 and Figure 5.

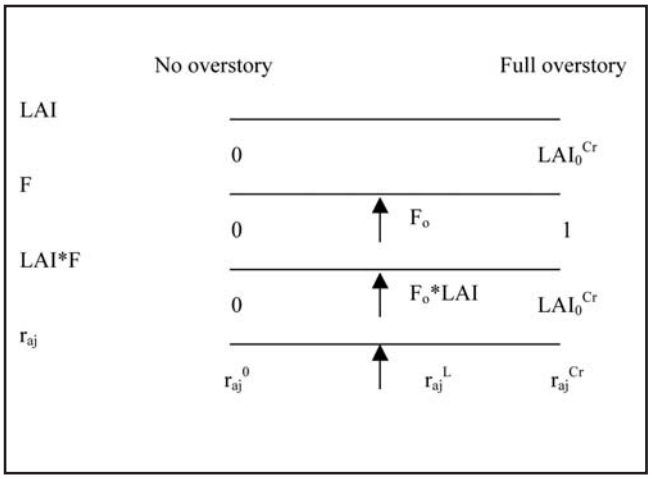

Figure 5. Schematic Showing Estimation Procedure of the Aerodynamic Resistance for Partial Canopy.

$$r_{aj}^{L} = \begin{cases} r_{aj}^{0} + \dfrac{LAI_o F_o}{LAI_o^{Cr}}(r_{aj}^{Cr} - r_{aj}^{0}) & \text{if } 0 \le LAI_o \le LAI_o^{Cr} \\ \mathrm{r_{aj}^{Cr}} & \text{if } LAI_o > LAI_o^{Cr} \end{cases} \tag{3.7.22}$$

where:

r_{aj}^{0} = aerodynamic resistances obtained for the case of no overstory from Equations 3.7.18 to 3.7.19 ($s.m^{-1}$),

r_{aj}^{Cr} = aerodynamic resistances obtained for the case of complete overstory from Equations 3.7.2 to 3.7.4 ($s.m^{-1}$),

LAI_o = LAI of the overstory varying in time and space (obtained from the growth model)($m^2.m^{-2}$),

LAI_o^{Cr} = threshold LAI of the overstory used to define a complete canopy cover ($m^2.m^{-2}$),

r_{aj}^{L} = aerodynamic resistance for the partial canopy ($s.m^{-1}$).

3.7.1.4 Aerodynamic Resistance with No Overstory and No Understory

In the case of no overstory and no understory, the aerodynamic resistance reduces to r_{ag} and is obtained using a logarithmic distribution as in Equation 3.7.23.

$$r_{ag} = r_{ag}^{a} = \frac{\left(\ln\left(\dfrac{Y}{z_{0g}}\right)\right)^2}{u(Y)k^2} \tag{3.7.23}$$

3.7.1.5 Aerodynamic Resistance with No Overstory and Partial Understory

Aerodynamic resistance is assumed to vary linearly with the product of understory LAI_u and ground cover (F_u) between the limits of fully developed understory and no understory. The aerodynamic resistances r_{aj} are first calculated for the fully developed understory (Section 3.7.1.2) and then for the case of no understory (Section 3.7.1.4). A linear interpolation is then performed as shown in Equation 3.7.22 and Figure 5.

3.7.2 Comparison with Pan Evaporation Data

Climate surface available for Australia includes pan evaporation data (Jeffrey *et al.*, 2001). The estimates of overstory, understory and soil evaporation demand from climate forcing are checked against the potential evapotranspiration data as shown below.

$$E_{to} + E_{tu} + E_{tg} \le P_{ET} \tag{3.7.24}$$

where:

P_{ET} = *coefficient* × *pan evaporation* ($m.s^{-1}$).

The coefficient for converting pan evaporation to potential evapotranspiration can either be constant or seasonally varying (Australian Bureau of Meteorology, 2001). If Equation 3.7.24 is not satisfied, then each of the evaporation demand is modified according to Equation 3.7.25.

$$E_{tj}^{new} = \frac{E_{tj}}{\sum_{j=1}^{3} E_{tj}} P_{ET} \tag{3.7.25}$$

where:

E_{tj}^{new} = modified evaporation demand ($m.s^{-1}$).

3.8 Pasture Growth Model (CLASS PGM)

Climatic variability across Australia where CLASS will be implemented varies from wet to arid, tropical, subtropical and temperate zones where seasonal rainfall dominance, temperature range and light intensity determine native pasture adaptation/ ecotype and constrain the choices of available crop type and exotic pastures adaptable to local catchment conditions. Therefore the pasture and crop growth models used need to be versatile enough to represent the complexity of multi-species and management interactions experienced across this wide range of climate but at the same time remain simple enough to represent this with a minimum number of parameters. The primary aim is to simulate the hydrologic response of species mix and management but also to provide broad estimates of agricultural productivity.

Broadly the plant physiological characteristics required to model agricultural pasture and crop management systems in a generic sense are whether the species are tropical or temperate (C4 or C3 species respectively), monocotoledonous (grasses) or dicotolydonous (broadleaf) species and whether they are perennial or annual. The need for the model to incorporate the season of growth (summer versus winter growth) and to simulate the feedback effects of grazing on plant growth and hydrologic fluxes are essential components of the plant growth module.

The pasture growth module is based on the work of Johnson (2003) and is adapted from Thornley and Johnson (2000) (see Johnson, 2003 for details). The following attributes can be handled generically by the model. This module is effective for Australian conditions while having relatively few parameters. Climatic inputs from Silo data (Jeffrey *et al.*, 2001) are adequate, and parameter responses to environment are consistent with such data.

The pasture growth model includes the following:

- Responses to light, temperature, evapotranspiration demand and soil water content.
- Shoot and root growth (dry weight) – shoot growth includes live and dead, leaf (LAI) and stem.
- A simple treatment for the response to soil salt content.
- A soil fertility factor is implemented that allows response to soil nutrient status to be incorporated, although plant nutrient status and demand are not specifically included at this stage.
- Pasture utilisation by grazing animals is described.
- Litter dynamics, which is particularly important in pastures, is addressed.
- The dependence of all parameters (where relevant) to climatic variables, soil water and salt status are included.
- Default parameters for generic species types are included.
- Methods for working with multiple species are included.
- The growth characteristics are based on carbon assimilation (photosynthesis and respiration), tissue turnover and senescence.
- The model includes above and below ground dry weight as well as shoot components: live, dead, leaf, stem, LAI. Canopy height is also included.
- The model for annual species does not include a seed bank – the simple approach used by Johnson (2003) is that the annual species will germinate only if the climatic conditions are suitable.

The following pasture species types are considered:

- Perennial or annual.
- C_3 or C_4.

Treatment for legumes is included although, in the absence of nutrients at this stage, it will not be entirely relevant. In addition, animal intake routines are incorporated although there is no specific treatment of animal growth. The only role of this component of the model is to utilise the pasture in a realistic manner.

3.9 Crop Growth Model (CLASS CGM)

Like the pasture growth module, the crop growth module is also based on the work of Johnson (2003) (see Johnson, 2003 for details). The crop module is developed for a range of species types, and the following are addressed.

- C_3 or C_4.
- Determinate or indeterminate (that is, whether leaf production and growth continues after the onset of flowering).
- Grain yield and LAI. Temporal variation of shoot and root dry weight, live and dead LAI, and grain yield are simulated.

Default parameter sets for generic species are included. Sowing schedule is an input to the model. The model includes germination, flowering and maturity (harvest), defined as dates. Although phase duration can be modelled in relation to climate, in a practical sense it is probably less reliable than just specifying dates.

3.10 Tree Growth Model (CLASS 3PG+)

3-PG+ (Morris, 2003), an adaptation of a generalised model of forest productivity using simplified concepts of radiation-use efficiency, carbon balance and its partitioning by Landsberg and Waring (1997) is used for modelling tree growth in CLASS. The model called Physiological Principles in Predicting Growth 3-PG, calculates total carbon fixed from utilisable, absorbed photosynthetically active radiation, obtained by correcting the photosynthetically active radiation absorbed by the forest canopy for the effects of drought, atmospheric vapour pressure deficits and stand age. A distinctive feature of this model is the treatment of the ratio of net and gross primary production as a constant and thus eliminating the need to estimate respiration to estimate net amount of carbon converted to biomass.

3-PG requires weather data as input, works on monthly time steps and can be used to simulate realistic patterns of stem growth and stem diameter increments. The simulation of leaf area index (LAI) is realistic for a range of soil conditions and atmospheric constraints.

3.11 Unsaturated Moisture Movement Model (CLASS U3M)

A local water balance is first performed for each pixel that takes into account gravity drainage, capillary rise, evapotranspiration and horizontal saturated inflow from the upslope areas. For each pixel located on the stream, inflow to the pixel is accumulated from overland and sub-surface pathways and no vertical flux computations are required. After local water balance is performed for each pixel on the land, excess moisture arising from saturated conditions within each soil material is then redistributed horizontally on the basis of multiple flow directions from the upslope contributing areas (Tarboton, 1997) and Darcy's law (Section 3.12). For a given time step and pixel location, water and solute balance computations are performed only after completing the vertical water and solute balance and horizontal redistribution for the same time step for all the upslope pixel that contribute to the pixel of interest. Vertical water balance can be performed at a shorter time step relative to the horizontal redistribution.

3.11.1 Mass Balance

Vertical water balance at a given pixel location p for a layered soil profile can be defined by Equation 3.11.1 (Figure 6). The surrounding eight pixel are denoted by k, k=0,1,….7 in clockwise direction beginning from upper left corner of the local domain (Figure 7).

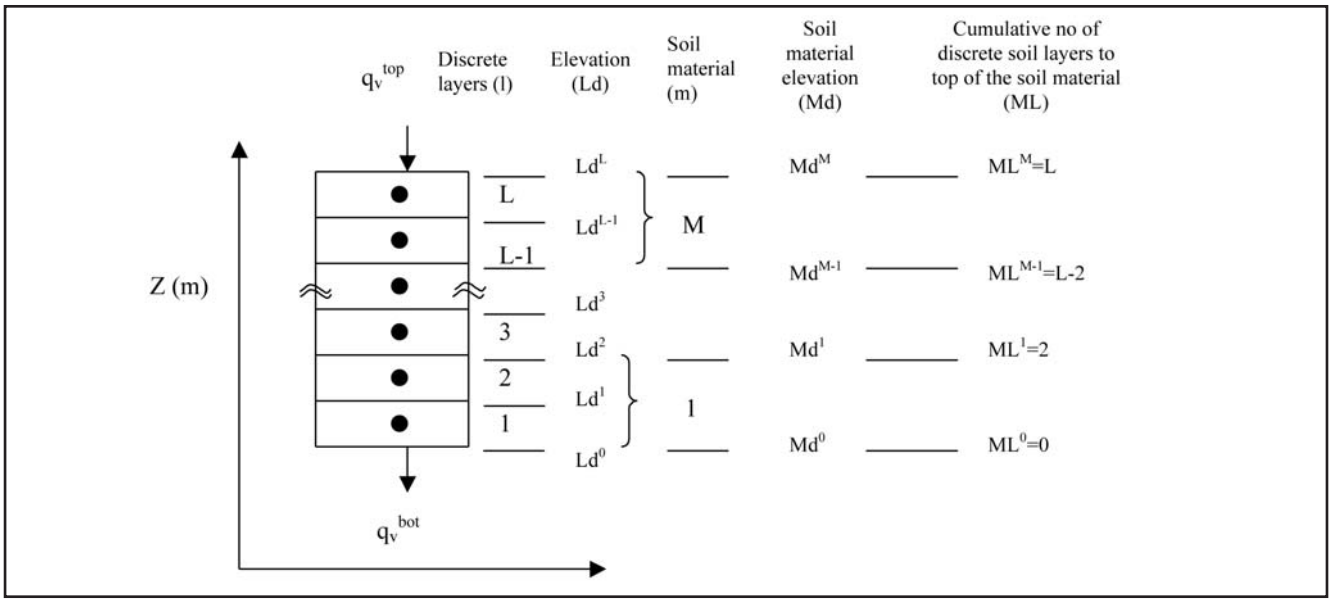

Figure 6. Schematic Diagram of the Soil Layer System with L Discrete Soil Layers and M Soil Materials.

$$\frac{\partial \theta(z,t)}{\partial t} = -\frac{\partial \vec{q}_v(z,t)}{\partial z} + S(z,t) \qquad (3.11.1)$$

where:

θ = volumetric water content ($m^3.m^{-3}$),

$\vec{q}_v$ = Darcy flux in the vertical direction ($m.s^{-1}$),

S = algebraic sum of the water sources and sinks expressed as volume of water per unit control volume per unit time (s^{-1}).

Darcy flux in the vertical direction can be written as in (3.11.2).

$$\vec{q}_v = -D(\theta)\frac{\partial \theta}{\partial z} - K_V(\theta) \qquad (3.11.2)$$

where:

$D(\theta) = K_V(\theta)/(d\theta/dh)$

= hydraulic diffusivity ($m^2.s^{-1}$),

$K_V(\theta)$ = unsaturated hydraulic conductivity along the vertical axis ($m.s^{-1}$).

Substituting Darcy flux from Equation 3.11.2 into Equation 3.11.1 results in the Richard's equation describing flow in the unsaturated zone (Richard, 1931). The source/sink term includes moisture loss by transpiration by the overstory and the understory, soil evaporation and moisture gain from the horizontal flow from the upslope areas (Equation 3.11.3).

where:

$E_{tj,a}$ = actual transpiration from the canopy j ($m.s^{-1}$)(minimum of the available soil moisture and climate demand; estimated from Equations 3.11.17 to 3.11.19),

$S_{E_{tj}}$ = actual transpiration from canopy j per unit control volume per unit time ($m^3.m^{-3}.s^{-1}$),

S_{E_s} = actual soil evaporation per unit control volume per unit time ($m^3.m^{-3}.s^{-1}$),

$b_j(z,t)$ = root biomass of the canopy *j* at depth z relative to the total root biomass (*dimensionless*)(estimated from the respective growth component),

$H_j(t)$ = rooting depth of the canopy *j* at time *t*,

Z = elevation of the soil surface with respect to mean sea level (m),

$E_{s,a}$ = actual soil evaporation ($m.s^{-1}$)(minimum of the available soil moisture and climate demand; estimated from Equation 3.11.20),

H_s = depth through which soil evaporation occurs (m),

$a_s(z)$ = proportion of the soil evaporation at depth z relative to the total soil evaporation (*dimensionless*),

w_{hor} = volume of water added (if any) from the upslope area per unit control volume per unit time ($m^3.m^{-3}.s^{-1}$) (estimated from the horizontal redistribution module).

$$S(z,t) = \begin{matrix} -S_{E_{tj}}(z,t) - S_{E_s}(z,t) + w_{hor}(z,t) & \text{when } Z - H_j(t) \le z \le Z, Z - H_s \le z \le Z \\ w_{hor}(z,t) & z \le Z - H_j(t) \text{ and } z \le Z - H_s \end{matrix} \qquad (3.11.3a)$$

$$E_{tj,a}(t) = \int_{Z-H_j(t)}^{Z} S_{E_{tj}}(z,t)dz = E_{tj,a}(t) \int_{Z-H_j(t)}^{Z} \frac{b_j(z,t)}{\int_{Z-H_j(t)}^{Z} b_j(z,t)dz} dz \qquad (3.11.3b)$$

$$E_{s,a}(t) = \int_{Z-H_s(t)}^{Z} S_{E_s}(z,t)dz = E_{s,a}(t) \int_{Z-H_s(t)}^{Z} \frac{a_s(z)}{\int_{Z-H_s(t)}^{Z} a_s(z)dz} dz \qquad (3.11.3c)$$

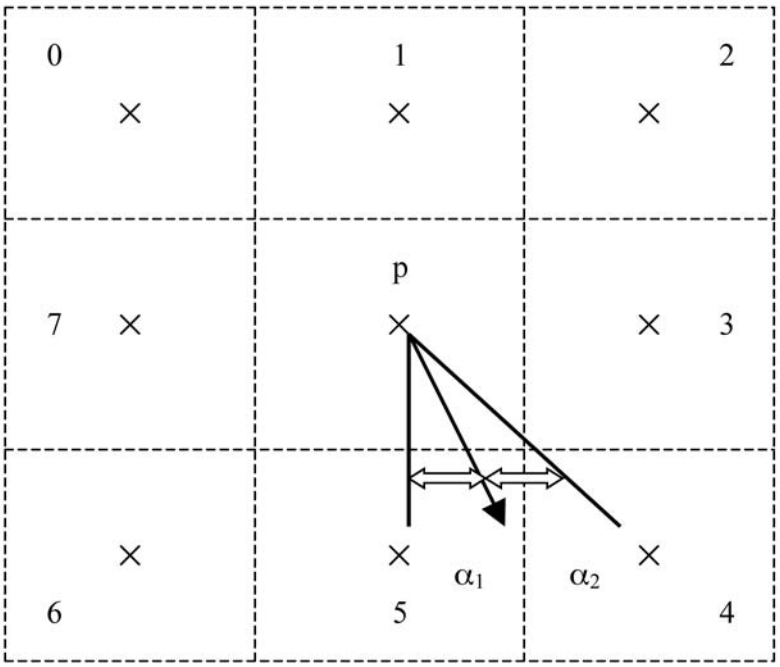

Figure 7. Schematic Diagram for Apportioning of the Flow δ^{pk} from Pixel p to Pixels 4 and 5. Flow direction is defined as the steepest downward slope on planar triangular facets on a block centred grid (Tarboton, 1997). Flow proportions δ^{p4} equals $\alpha_1/(\alpha_1+\alpha_2)$ and δ^{p5} equals $\alpha_2/(\alpha_1+\alpha_2)$.

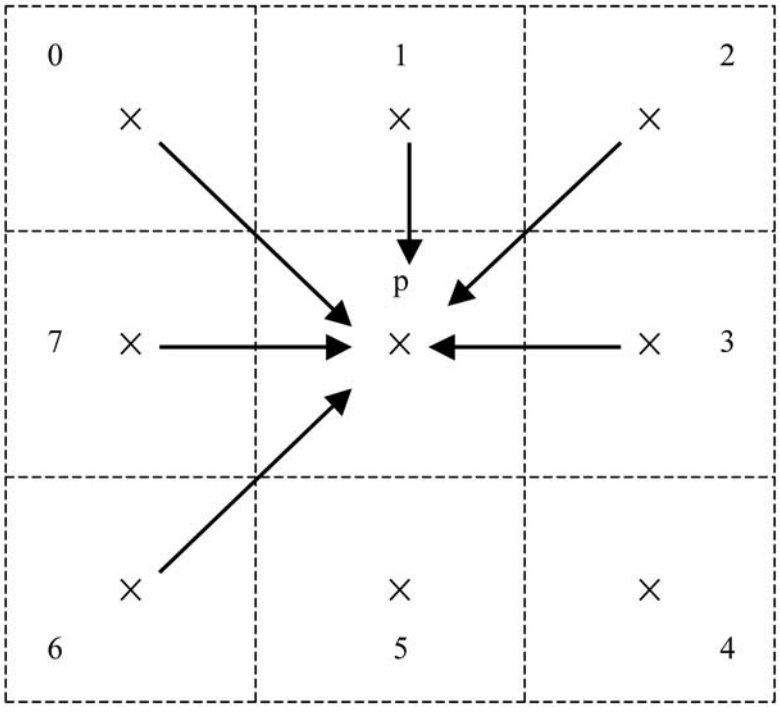

Figure 8. Schematic Diagram Showing Accumulation of the Flow from Upslope Pixels 0, 1, 2, 3, 6 and 7 to Pixel P. Flow direction from (Tarboton, 1997) and Darcy's law are used to describe the upslope boundary condition.

3.11.2 Boundary Conditions

Upper Boundary Condition

Neumann Type II time dependent specified flux upper boundary condition ($q_v^{top}\ m.s^{-1}$) is used at the soil surface (Equation 3.11.4a). Overland flow from upslope pixel k to the given pixel p is included in the flux available at the soil surface for infiltration (Figure 7) (Equation 3.11.4b). Moisture that cannot infiltrate into the soil is transferred to the downslope pixel k as the overland flow (Equations 3.11.4c to 3.11.4f).

$$q_v^{top}(t) = -\min\left(I_{cap}(t), P(t) + q_{o,in}(t)\right) \quad (3.11.4a)$$

$$q_{o,in}(t) = q_o^p(t) \quad (3.11.4b)$$

$$q_{o,out}(t) = \max\left(0, P(t) + q_{o,in}(t) - I_{cap}(t)\right) \quad (3.11.4c)$$

$$q_o^{pk}(t) = q_{o,out}(t)\delta^{pk} \quad (3.11.4d)$$

$$\sum_{k=0}^{7} \delta^{pk} = 1 \quad (3.11.4e)$$

$$q_o^k(t) = q_o^k(t) + q_o^{pk}(t) \quad (3.11.4f)$$

where:

$q_{o,in}$ = total incoming overland flow contribution from all upslope pixels ($m.s^{-1}$),

$q_{o,out}$ = total outgoing overland flow contribution to all downslope pixels ($m.s^{-1}$),

P = Precipitation throughfall at the soil surface after accounting for the canopy interception ($m.s^{-1}$)(equals P_o when overstory is present with no understory – from Equation 3.5.5; equals P_u if understory is present – from Equation 3.5.8; and equals precipitation P in the case of bare soil),

I_{cap} = Infiltration capacity at the soil surface ($m.s^{-1}$)(estimated from 3.6.1),

q_o^p and q_o^k = overland flow received at pixels p and k respectively from upslope pixels at the current time step ($m.s^{-1}$),

q_o^{pk} = overland flow from pixel p to k ($m.s^{-1}$),

δ^{pk} = proportion of the overland flow from pixel p to k (*dimensionless*) (estimated from Tarboton, 1997: Figure 7).

Lower Boundary Condition

A separate boundary condition is used for the recharge and the discharge areas on the land. Discharge areas on the land can be identified a priori either from known areas affected by shallow water table or from the FLAG model (Roberts *et al.*, 1997; Summerell *et al.*, 2003) or both.

In the recharge areas, flux from the lower boundary ($q_v^{bot}\ m.s^{-1}$) is taken as minimum of the flux under unit gradient from the bottom soil layer and hydraulic conductivity of the sub-surface material. Recharge areas are defined as locations where a proportion of the drainage from the soil profile contributes to groundwater as recharge.

$$q_v^{bot}(t) = -\min\left(K_V\left(\theta^1(t)\right), K_{sub}\right) \quad (3.11.5a)$$

$K_V\left(\theta^1(t)\right)$ = unsaturated hydraulic conductivity of the bottom layer along the vertical axis ($m.s^{-1}$),

D = depth of the soil profile model domain (m),

K_{sub} = saturated hydraulic conductivity of the sub-surface underneath the soil profile ($m.s^{-1}$).

In the discharge areas, a specified flux boundary condition is used (Equation 3.11.5b). Upward flux through the lower boundary for each pixel in the discharge zone is calculated according to the methodology described in Section 3.14.2. If upward flux in the discharge area is zero (no contribution from the upslope area) then free drainage is assumed to occur below the modelled soil domain.

$$q_v^{bot}(t) = \begin{cases} Q_v^{bot,p}(t) & \text{if } Q_v^{bot,p}(t) > 0 \\ -\min\left(K_V\left(\theta^1(t)\right), K_{sub}\right) & \text{if } Q_v^{bot,p}(t) = 0 \end{cases} \quad (3.11.5b)$$

where:

$Q_v^{bot,p}$ = upward flux from bottom of the soil profile at pixel p in the discharge zone ($m.s^{-1}$) (estimated from Equation 3.14.18).

Negative sign on the right hand side of Equations 3.11.4a and 3.11.5a indicates that flux is opposite to the z-axis whereas flux in the discharge zone is along the z-axis (Equation 3.11.5b).

Upslope Boundary Condition

Horizontal transfers are assumed to occur between the respective soil material from the upslope pixel k to the downslope pixel p (e.g. from the topmost soil material M_k at k to the topmost soil material M_p at p) (Figure 8). System dependent subsurface saturated inflow from the soil material m_k of all the upslope pixel k into the soil material m_p at pixel p is estimated as in Equation 3.11.6.

$$W_{in}^{m_p,p}(t) = \frac{Q_{hor}^{m_p,p}(t)}{Md(m_p) - Md(m_p - 1)} \qquad (3.11.6)$$

where:

$W_{in}^{m_p,p}$ = volume of water per unit control volume received either as horizontal subsurface flow into the soil material m_p from the soil material m_k of all the upslope pixel k or excess moisture remaining at the end of previous time step that could not be transferred horizontally to the neighbouring downslope pixels or both ($m^3.m^{-3}$)(see Section 3.12),

$Q_{hor}^{m_p,p}$ = volume of water added as subsurface flow into the soil material m_p at pixel p from the soil material m_k at all upslope pixels k (m) (expressed as depth of water and is obtained from Equations 3.12.4j to 3.12.4l, using flow directions and Darcy's law),

$Md(m_p)$= elevation at top of the soil material m_p at $p(m)$,

M_p = maximum number of soil materials at pixel p (*dimensionless*),

M_k = maximum number of soil materials at pixel k (*dimensionless*). The relationship between m_p and m_k is such that when m_p equals $M_p - j$, m_k equals $M_k - j$, for all $j = 0,1,2...j\max$ and $j\max$ equals $M_p - 1$ when $M_k > M_p$ and $M_k - 1$ when $M_k \leq M_p$.

All computations proceed from upslope to downslope areas and therefore all upslope contributions are considered at the current time step.

3.11.3 Numerical Solution

The discrete soil layers $i = 1,2,3....L$ belong to the soil material $m = 1,2,3....M$ (Figure 6). Elevation to the top of each discrete soil layer is denoted by Ld^i and the elevation to the top of each soil material is denoted by Md^m. Cumulative number of discrete soil layers up to the top of each soil material m is denoted by ML^m (i.e. $ML^M = L$ for the complete soil profile).

The finite difference numerical approximation of Equation 3.11.1 for a pre-defined layered soil system ($i = 1,2....L$) at pixel p can be written as in Equation 3.11.7. To allow for better accuracy of the numerical solution, vertical flux computations are implemented at a shorter time interval $\delta t'$ compared to the time interval δt required for horizontal redistribution as described in Section 3.12. When an integer multiple J ($= \delta t/\delta t'$) times $\delta t'$ equals δt during simulations, vertical flux computations are stopped and horizontal flux transfers are calculated. Therefore time $t+\delta t$ equals $t+\delta t'$ and any time step for the vertical flux computations can be defined as $t+j\delta t'$, $j = 1,2,.....,J$ (see Equation 3.11.7 below).

where:

w_{tj}^i and w_s^i represent the transpiration and soil evaporation terms respectively (Equations 3.11.8 to 3.11.9),

w_q^i represents the volume flux term (Equation 3.11.10),

w_{hor}^i represents the saturated subsurface horizontal flux term (Equation 3.11.11),

$\delta t'$ represents the time interval for local mass balance (s) and

δt represents the time interval for horizontal redistribution (s).

All terms inside the bracket on the right hand side of Equation 3.11.7 represent volume of water per unit control volume per unit time ($m^3.m^{-3}s^{-1}$).

$$\theta^i(t + j\delta t') = \theta^i(t + (j-1)\delta t') + \left(-w_q^i - w_{tj}^i - w_s^i + w_{hor}^i\right)\delta t' \qquad (3.11.7)$$

$$w_{tj}^{i}(t+j\delta t') = \frac{E_{tj}(t+j\delta t')}{\delta z^{i}} \frac{b_j^i}{\sum_{k=1}^{L} b_j^k} \qquad (3.11.8)$$

$$w_{s}^{i}(t+j\delta t') = \frac{E_{s}(t+j\delta t')}{\delta z^{i}} \frac{a_s^i}{\sum_{k=1}^{L} a_s^k} \qquad (3.11.9)$$

$$w_{q}^{i}(t+j\delta t') = \left(\frac{q_v^{i+\frac{1}{2}} - q_v^{i-\frac{1}{2}}}{\delta z^{i}} \right)_{t+(j-1)\delta t'} \qquad (3.11.10)$$

$$w_{hor}^{i}(t+j\delta t') = \frac{W_{in}^{m_p,p}(t+j\delta t')}{\delta t'} \qquad (3.11.11)$$

where:

L = total number of the discrete soil layers,

$E_{tj}(t+j\delta t') = E_{tj}(t+\delta t)$

= canopy transpiration demand over the time step $t + \delta t$ obtained from Equation 3.7.1 ($m.s^{-1}$),

$E_s(t+j\delta t') = E_s(t+\delta t)$

= soil evaporation demand over the time step $t + \delta t$ obtained from Equation 3.7.1 ($m.s^{-1}$),

$W_{in}^{m_p,p}(t+j\delta t') = \frac{W_{in}^{m_p,p}(t)}{J}$

= volume of water per unit control volume received as inflow over the time step $\delta t'$ ($m^3.m^{-3}$),

$J = \delta t / \delta t'$

= number of time steps for the vertical mass balance within a single time step for horizontal redistribution (-).

Plant transpiration demand from the canopy E_{tj}^{i} and the soil evaporation demand E_s are available from climate forcing for the time $t + \delta t$ (3.7.1). Computations for a given pixel p are performed only after computations for all the upslope pixels that contribute to p are completed. Therefore volume of water added to pixel p as horizontal saturated flow $W_{in}^{m_p,p}(t+\delta t)$ from all the upslope pixels k, is available from Equation 3.11.6 at the end of current time step of the horizontal transfers (Equation 3.11.11).

Ideally spatial derivative of the Darcy's flux w_q^i along the vertical should be considered at time $t + j\delta t'$ i.e. implicit solution of the Richard's equation. However, for a catchment based modelling system, computational requirements would be too much. Therefore, the term w_q^i is considered at time $t + (j-1)\delta t'$ (Equations 3.11.12 to 3.11.13) i.e. explicit solution of Equation 3.11.7. When the time step $\delta t'$ for the vertical water balance is small relative to the horizontal re-distribution time step δt, the solution approaches the implicit solution of Equation 3.11.1 and the numerical simulation times are likely to be large.

Moisture contents are considered at the node. Hydraulic conductivity and diffusivity are considered at the interface of the adjoining discrete soil layers and are expressed as geometric mean of the respective values (see Equations 3.11.12 and 3.11.13 below).

where:

$q_v^{top}(t+j\delta t') = q_v^{top}(t+\delta t)$

= infiltration from the soil surface from Equation 3.11.4a ($m.s^{-1}$),

$q_v^{bot}(t+j\delta t')$

= flux from bottom of the soil profile over the time step $t + j\delta t'$ from Equations 3.11.5a to 3.11.5b ($m.s^{-1}$).

$$q_v^{i+\frac{1}{2}}(t+j\delta t') = \begin{cases} \left(-\sqrt{D(\theta^{i+1})D(\theta^{i})} \frac{\theta^{i+1}-\theta^{i}}{\delta z^{i}} - \sqrt{K_V(\theta^{i+1})K_V(\theta^{i})} \right)_{t+(j-1)\delta t'} & \text{if } 1 \le i < L \\ q_v^{top}(t+j\delta t') & \text{if } i = L \end{cases} \qquad (3.11.12)$$

$$q_v^{i-\frac{1}{2}}(t+j\delta t') = \begin{cases} \left(-\sqrt{D(\theta^{i})D(\theta^{i-1})} \frac{\theta^{i}-\theta^{i-1}}{\delta z^{i}} - \sqrt{K_V(\theta^{i})K_V(\theta^{i-1})} \right)_{t+(j-1)\delta t'} & \text{if } 1 < i \le L \\ q_v^{bot}(t+j\delta t') & \text{if } i = 1 \end{cases} \qquad (3.11.13)$$

To avoid an iterative procedure for solution of Equation 3.11.7 we first distribute the moisture vertically by taking into account infiltration from the soil surface and horizontal saturated flow from all the upslope pixels to estimate $\theta^i_{temp}(t + j\delta t')$ (ie. ignoring w^i_{tj} and w^i_s in 3.11.7). If estimated soil moisture content is less than the residual soil moisture content θ^i_r then it is constrained to θ^i_r (Equation 3.11.14a) and the Darcy's flux is adjusted accordingly (Equation 3.11.14b). Simulation proceeds from the uppermost soil layer down to the deeper soil layers (see Equations 3.11.14a and 3.11.14b below).

After vertical moisture distribution we remove moisture by soil evaporation and plant transpiration (Equations 3.11.15 to 3.11.20). Soil moisture is permitted to vary between the residual and the saturated soil moisture content during evapotranspiration computations.

The available soil moisture after drainage (W^i_{avail} in $m^3.m^{-3}$) can be expressed as in Equation 3.11.15 and total evapotranspiration demand from climate forcing while accounting for moisture, salinity and temperature stresses through the Penman Monteith equation (W^i_{ET} in $m^3.m^{-3}$) during the time step $t + \delta t$ can be expressed as in Equation 3.11.16. Actual evapotranspiration from the layer (W^i_{tjs} in $m^3.m^{-3}$) is taken as minimum of the two terms (Equation 3.11.17). Note that lower case *w* represents the volume of water per unit control volume per unit time. However, upper case *W* represents the volume of water per unit control volume i.e. integral of the rate *w* over the time step (See Equations 3.11.15 to 3.11.17 below).

Actual transpiration and soil evaporation from the soil layer *i* after accounting for soil moisture availability can now be estimated as in Equations 3.11.18 to 3.11.20.

$$W^i_{to}(t + j\delta t') = \frac{w^i_{to}(t + j\delta t')\delta t'}{W^i_{ET}(t + j\delta t')} W^i_{tjs}(t + j\delta t') \tag{3.11.18}$$

$$W^i_{tu}(t + j\delta t') = \frac{w^i_{tu}(t + j\delta t')\delta t'}{W^i_{ET}(t + j\delta t')} W^i_{tjs}(t + j\delta t') \tag{3.11.19}$$

$$W^i_{s}(t + j\delta t') = \frac{w^i_{s}(t + j\delta t')\delta t'}{W^i_{ET}(t + j\delta t')} W^i_{tjs}(t + j\delta t') \tag{3.11.20}$$

$$\theta^i_{temp}(t + j\delta t') = \max\left(\theta^i_r, \theta^i(t + (j-1)\delta t') + \left(- w^i_q(t + j\delta t') + w^i_{hor}(t + j\delta t')\right)\delta t'\right) \tag{3.11.14a}$$

$$\text{If } \theta^i_{temp}(t + j\delta t') = \theta^i_r \text{ then } \begin{aligned} w^i_{q,new} &= \left(\theta^i(t + (j-1)\delta t') - \theta^i_r + w^i_{hor}\delta t'\right)/\delta t' \\ q_v^{i+\frac{1}{2}}(t + (j-1)\delta t') &= q_v^{i+\frac{1}{2}}(t + (j-1)\delta t')\frac{w^i_{q,new}}{w^i_q} \\ q_v^{i-\frac{1}{2}}(t + (j-1)\delta t') &= q_v^{i-\frac{1}{2}}(t + (j-1)\delta t')\frac{w^i_{q,new}}{w^i_q} \end{aligned} \tag{3.11.14b}$$

$$W^i_{avail}(t + j\delta t') = \max\left(0, \theta^i_{temp}(t + j\delta t') - \theta^i_r\right) \tag{3.11.15}$$

$$W^i_{ET}(t + j\delta t') = \left(w^i_{to}(t + j\delta t') + w^i_{tu}(t + j\delta t') + w^i_s(t + j\delta t')\right)\delta t' \tag{3.11.16}$$

$$W^i_{tjs}(t + j\delta t') = \min\left(W^i_{ET}(t + j\delta t'), W^i_{avail}(t + j\delta t')\right) \tag{3.11.17}$$

When W^i_{tjs} equals W^i_{ET}, evapotranspiration demand estimated from Penman Monteith equation is completely satisfied (atmospheric control). However, when W^i_{tjs} is less than W^i_{ET}, moisture availability determines the evapotranspiration amounts (soil control). Soil moisture is then adjusted depending on water loss by evapotranspiration (Equation 3.11.21). If the estimated soil moisture content for any soil layer is greater than the saturated soil moisture content θ^i_s then it is constrained to the saturated soil moisture content and excess moisture is computed (Equation 3.11.22).

Total transpiration, soil evaporation and excess moisture is then accumulated for each soil layer over the horizontal transfer time step δt as in Equation 3.11.23.

$$\begin{aligned} W^i_{to}(t+\delta t) &= \sum_{j=1}^{J} W^i_{to}(t+j\delta t') \\ W^i_{tu}(t+\delta t) &= \sum_{j=1}^{J} W^i_{tu}(t+j\delta t') \\ W^i_{s}(t+\delta t) &= \sum_{j=1}^{J} W^i_{s}(t+j\delta t') \\ \theta^i_{ex}(t+\delta t) &= \sum_{j=1}^{J} \theta^i_{ex}(t+j\delta t') \end{aligned} \qquad (3.11.23)$$

Drainage from the soil profile and flux across the bottom of each soil material is accumulated over the time step $t + \delta t$ as in Equation 3.11.24.

where:

$Q^{m_p,p}_{bot}(t+\delta t)$ = flux at the bottom of the soil material m_p at p over the horizontal re-distribution time step (m).

Flux across the top of each soil material is accumulated over the time step $t + \delta t$ as in Equation 3.11.25.

where:

$Q^{m_p,p}_{top}(t+\delta t)$ = flux across the top of the soil material m_p at p over the horizontal re-distribution time step (m).

3.12 Horizontal Redistribution and Sub-surface Flow from each Soil material

Soil moisture in excess of the moisture holding capacity for each discrete soil layer is accumulated over the respective soil material and is transferred as sub-surface flow to the two downslope pixels according to the multiple flow direction algorithm of Tarboton (1997) and Darcy's law. Horizontal transfers occur over the time interval δt.

The sub-surface flow routing model is adapted from a grid based quasi three-dimensional model of Wigmosta and Lettenmaier (1997). An important difference between the approach of these authors and the popularly used statistical dynamical approach originally proposed by Beven and Kirkby (1979) is the use of grid cells as against the use of hydrological similarity concepts. The hydrological similarity concept or the wetness index, while numerically very simple, is not suitable for predicting the effects of landuse change which is the primary objective of CLASS. For practical reasons landuse changes are invariably required at the property level and the objective is not to just predict the impact of landuse changes at the catchment outlet but also to quantify the downslope landscape impacts. Many different landscape elements in the catchment can have same wetness index. This produces difficulties in implementing landuse change scenarios.

$$\theta^i(t+j\delta t') = \min\left(\theta^i_s, \theta^i_{temp}(t+j\delta t') - W^i_{tjs}(t+j\delta t')\right) \qquad (3.11.21)$$

$$\theta^i_{ex}(t+j\delta t') = \max\left(0, \left(\theta^i_{temp}(t+j\delta t') - W^i_{tjs}(t+j\delta t')\right) - \theta^i_s\right) \qquad (3.11.22)$$

$$Q^{m_p,p}_{bot}(t+\delta t) = \begin{cases} \sum_{j=1}^{J} q^{bot}_v(t+j\delta t')\delta t' & \text{if } m_p = 1 \\ \sum_{j=1}^{J} q^{ML(m_p-1)+1/2}_v(t+j\delta t')\delta t' & \text{if } 1 < m_p \le M_p \end{cases} \qquad (3.11.24)$$

$$Q^{m_p,p}_{top}(t+\delta t) = \begin{cases} \sum_{j=1}^{J} q^{top}_v(t+j\delta t')\delta t' & \text{if } m_p = M_p \\ \sum_{j=1}^{J} q^{ML(m_p)+1/2}_v(t+j\delta t')\delta t' & \text{if } 1 \le m_p < M_p \end{cases} \qquad (3.11.25)$$

The excess moisture content $\theta_{ex}^{i}(t+\delta t)$ from Equation 3.11.23 of the discrete soil layers is pooled over the respective soil material depth to estimate the total excess moisture over the soil material (Equation 3.12.1). Material soil moisture is then estimated (Equation 3.12.2). A perched water table is created separately for each material when proportional soil moisture becomes unity (Equation 3.12.3).

Total excess soil moisture in each soil material m_p at p can be estimated as depth of water as in Equation 3.12.1.

$$d_{ex}^{m_p,p}(t+\delta t) = \sum_{i=ML(m_p-1)+1}^{ML(m_p)} \theta_{ex}^{i}(t+\delta t)\delta z^{i} \qquad (3.12.1)$$

where:

$d_{ex}^{m_p,p}$ = moisture in excess of saturated moisture-holding capacity in the soil material m_p (m).

Soil moisture over the soil material ($m^3.m^{-3}$) and the proportional soil material saturation $P_{sat}^{m_p,p}$ (*dimensionless*) are estimated as in Equations 3.12.2 and 3.12.3 respectively.

$$\theta^{m_p,p}(t+\delta t) = \frac{\sum_{i=ML(m_p-1)+1}^{ML(m_p)} \theta^{i}(t+\delta t)\delta z^{i}}{Md(m_p) - Md(m_p-1)} \qquad (3.12.2)$$

$$P_{sat}^{m_p,p}(t+\delta t) = \frac{\theta^{m_p,p}(t+\delta t)}{\theta_{s}^{m_p,p}} \qquad (3.12.3)$$

Letting n_d denote the number of downslope pixels k,k = 0,1,2,....,7 with non-zero flow weight ($\delta^{pk} > 0$), its value equals 1 for the D8 method and equals either 1 or 2 for the D∞ method (Tarboton, 1997). The soil materials 1,2,.....,M_p at pixel p and 1,2,.....,M_k at k are numbered from the bottom (Figure 6). Saturated horizontal transfers are permitted between the respective soil materials from the top i.e. M_p to M_k, $M_p - 1$ to $M_k - 1$ etc. Since the number of soil materials M_p at p and M_k at k can be different, therefore mapping of a given soil material m_p at p to the respective soil material m_k at k is required as in (3.12.4a).

$$m_k = \max\left(1, M_k - (M_p - m_p)\right) \qquad (3.12.4a)$$

For each downslope pixel k with non-zero flow weight (1,2,...,n_d), calculate the *available* soil moisture for horizontal transfer from soil material m_p at p to the respective soil material m_k at k (Equation 3.12.4b) and also from Darcy's law (Equations 3.12.4c to 3.12.4i).

$$A_{hor}^{m_p,pk}(t+\delta t) = d_{ex}^{m_p,p}(t+\delta t)\delta^{pk} \qquad (3.12.4b)$$

$$K_H^{m_p,p}(t+\delta t) = K_H^{m_p,p}\left(\theta^{m_p,p}(t+\delta t)\right) \qquad (3.12.4c)$$

$$K_H^{m_k,k}(t) = K_H^{m_k,k}\left(\theta^{m_k,k}(t)\right) \qquad (3.12.4d)$$

$$\overline{K}_H = \sqrt{K_H^{m_p,p}(t+\delta t)K_H^{m_k,k}(t)} \qquad (3.12.4e)$$

$$h^{m_p,p}(t+\delta t) = h^{m_p,p}\left(\theta^{m_p,p}(t+\delta t)\right) \qquad (3.12.4f)$$

$$h^{m_k,k}(t) = h^{m_k,k}\left(\theta^{m_k,k}(t)\right) \qquad (3.12.4g)$$

(See Equations 3.12.4h and 3.12.4i below)

where:

$A_{hor}^{m_p,pk}$ = moisture available for horizontal transfer from the soil material m_p at p to the respective soil material m_k at k (m),

$q_{hor}^{m_p,pk}$ = moisture that can be transferred horizontally using Darcy's law from the soil material m_p at p to the respective soil material m_k at k (m),

θ = soil moisture ($m^3.m^{-3}$),

$K_H = K_V / IK^A$ = unsaturated hydraulic conductivity along the horizontal axis ($m.s^{-1}$),

IK^A = anisotropy ratio (-),

$$q_{hor}^{m_p,pk}(t+\delta t) = \max\left\{0, -\overline{K}_H\left(\frac{h^{m_k,k}(t) - h^{m_p,p}(t+\delta t)}{\delta S} + \frac{Z^{k} - Z^{p}}{\delta S}\right)\delta t\right\} \qquad (3.12.4h)$$

$$D_{ex}^{m_p,pk}(t+\delta t) = A_{hor}^{m_p,pk}(t+\delta t) + \text{unused } D_{ex} - q_{hor}^{m_p,pk}(t+\delta t) \qquad (3.12.4i)$$

h = pressure head (m),

$D_{ex}^{m_p,pk}$ = difference between moisture available for horizontal transfer and moisture that can be transferred from soil material m_p at p to the respective soil material m_k at k (m),

δS = distance between the centre of pixel p and k (m).

A lower bound is introduced in Equation 3.12.4h to ensure that excess moisture gets to the stream eventually in the areas of low relief.

The variable $D_{ex}^{m_p,pk}$ can take a positive, negative or a zero value (Equation 3.12.4i). A positive value indicates that Darcy's flux is the limiting case whereas a negative value indicates that moisture availability is the limiting case. A zero value indicates balance between the available moisture and the moisture that can be transferred from the soil material m_p at p to the respective soil material m_k at k.

Case 1

For each downslope pixel k with non-zero flow weight (n_d pixels with $\delta^{pk}>0$) that have $D_{ex}^{m_p,pk} \geq 0$, calculate actual horizontal soil moisture transfer from m_p at p to m_k at k using Equation 3.12.4j. Maintain a record of all inflow coming into the soil material m_k at k and depletion of the excess moisture from the soil material m_p at p (see Equation 3.12.4j below).

where:

$d_{hor}^{m_p,pk}$ = actual horizontal soil moisture transfer from the soil material m_p at p to m_k at k (m),

$Q_{hor}^{m_k,k}(t+\delta t)$ = inflow coming into the soil material m_k at pixel k from all neighbouring upslope pixels with $\delta^{pk}>0$(m),

$Q_{hor,out}^{m_p,p}(t+\delta t)$ = total horizontal outflow from the soil material m_p at p to the neighbouring downslope pixels during the time step $t+\delta t$ (m).

Case 2

For each downslope pixel k with non-zero flow weight (n_d pixels with $\delta^{pk} > 0$) that have $D_{ex}^{m_p,pk} < 0$, calculate actual horizontal soil moisture transfer from m_p at p to m_k at k using Equation 3.12.4k. Equation 3.12.4k can be applied ONLY so long as some excess soil moisture is available for horizontal transfer ($d_{ex}^{m_p,p}(t+\delta t) \geq 0$) (see Equation 3.12.4k below).

If solute transport is simulated, Equations 4.1.7 to 4.1.8 must be estimated after estimating Equations 3.12.4j to 3.12.4k.

If some excess moisture is still available in the soil material m_p at p ($d_{ex}^{m_p,p} > 0$) after performing (Equations 3.12.4j to 3.12.4k), then this moisture is made available for vertical drainage and evapotranspiration at the next time step (Equation 3.12.4l) (see upslope boundary condition Equation 3.11.6). This step should be performed just before computation for this pixel is finished.

$$Q_{hor}^{m_p,p}(t+\delta t) = \begin{cases} d_{ex}^{m_p,p}(t+\delta t) & \text{if } d_{ex}^{m_p,p}(t+\delta t) > 0 \\ 0 & \text{if } d_{ex}^{m_p,p}(t+\delta t) = 0 \end{cases} \quad (3.12.4l)$$

$$\text{If } D_{ex}^{m_p,pk}(t+\delta t) \geq 0 \begin{cases} d_{hor}^{m_p,pk}(t+\delta t) = q_{hor}^{m_p,pk}(t+\delta t) \\ Q_{hor}^{m_k,k}(t+\delta t) = Q_{hor}^{m_k,k}(t+\delta t) + d_{hor}^{m_p,pk}(t+\delta t) \\ d_{ex}^{m_p,p}(t+\delta t) = d_{ex}^{m_p,p}(t+\delta t) - d_{hor}^{m_p,pk}(t+\delta t) \\ Q_{hor,out}^{m_p,p}(t+\delta t) = Q_{hor,out}^{m_p,p}(t+\delta t) + d_{hor}^{m_p,pk}(t+\delta t) \\ \text{unused } D_{ex} = D_{ex}^{m_p,pk} \end{cases} \quad (3.12.4j)$$

$$\text{If } D_{ex}^{m_p,pk}(t+\delta t) < 0 \begin{cases} d_{hor}^{m_p,pk}(t+\delta t) = \min\left(d_{ex}^{m_p,p}(t+\delta t), A_{hor}^{m_p,pk}(t+\delta t)\right) \\ Q_{hor}^{m_k,k}(t+\delta t) = Q_{hor}^{m_k,k}(t+\delta t) + d_{hor}^{m_p,pk}(t+\delta t) \\ d_{ex}^{m_p,p}(t+\delta t) = \max\left(0, d_{ex}^{m_p,p}(t+\delta t) - d_{hor}^{m_p,pk}(t+\delta t)\right) \\ Q_{hor,out}^{m_p,p}(t+\delta t) = Q_{hor,out}^{m_p,p}(t+\delta t) + d_{hor}^{m_p,pk}(t+\delta t) \end{cases} \quad (3.12.4k)$$

In computing Equations 3.12.4a to 3.12.4k, horizontal transfer of excess moisture is done for the first soil material ($m_p = 1$) at p to all downslope pixels k (n_d pixels with $\delta^{pk}>0$). Thereafter soil materials are taken up sequentially (Equations 3.12.4a to 3.12.k) and computations are performed.

3.13 Soil Material Water Balance

A material water balance for pixel p is conducted by expressing all fluxes over the time step and soil moisture storage as depth of water (m).

Actual soil evaporation and the overstory and understory plant transpiration over each soil material are estimated using Equations 3.13.1 to 3.13.2 respectively.

$$E_{s,a}^{m_p,p}(t+\delta t) = \sum_{i=ML(m_p-1)+1}^{ML(m_p)} W_s^i(t+\delta t)\delta z^i \qquad (3.13.1)$$

$$E_{tj,a}^{m_p,p}(t+\delta t) = \sum_{i=ML(m_p-1)+1}^{ML(m_p)} W_{tj}^i(t+\delta t)\delta z^i \qquad (3.13.2)$$

where:

$E_{s,a}^{m_p,p}$ = actual soil evaporation from the soil material m_p (m),

$E_{tj,a}^{m_p,p}$ = actual transpiration from the soil material m_p and canopy j (m).

Total horizontal inflow to the soil material and outflow from the soil material is estimated as in Equations 3.13.3 and 3.13.4 respectively.

$$Q_{in}^{m_p,p}(t+\delta t) = Q_{hor}^{m_p,p}(t+\delta t) \qquad (3.13.3)$$

$$Q_{out}^{m_p,p}(t+\delta t) = Q_{hor,out}^{m_p,p}(t+\delta t) \qquad (3.13.4)$$

where:

$Q_{in}^{m_p,p}$ = total horizontal saturated subsurface inflow into the material m_p during the time step (obtained from upslope areas at the beginning of current time step)(m) (Equations 3.12.4j to 3.12.4k),

$Q_{out}^{m_p,p}$ = total horizontal saturated subsurface outflow from the material m_p during the current time step (m) (Equations 3.12.4j to 3.12.4k).

Total vertical flow $Q_{bot}^{m_p,p}$ (m) from bottom of the soil material and $Q_{top}^{m_p,p}$ (m) from top of the soil material are estimated from Equations 3.11.24 and 3.11.25 respectively.

Actual available soil moisture storage for each material S_{m_p} (m) is obtained from Equations 3.13.5 to 3.13.6.

$$S_{m_p}^p(t) = \sum_{i=ML(m_p-1)+1}^{ML(m_p)} \theta^i(t)\delta z^i \qquad (3.13.5)$$

$$S_{m_p}^p(t+\delta t) = \sum_{i=ML(m_p-1)+1}^{ML(m_p)} \theta^i(t+\delta t)\delta z^i \qquad (3.13.6a)$$

$$P_{sat}^{m_p,p}(t+\delta t) = \frac{S_{m_p}^p(t+\delta t)}{\left(Md(m_p) - Md(m_p-1)\right)\theta_s^{m_p}} \qquad (3.13.6b)$$

where:

$P_{sat}^{m_p,p}(t+\delta t)$ = proportional soil moisture saturation (-).

Estimated soil moisture storage and proportional water balance error are estimated from Equations 3.13.7 and 3.13.8 respectively. The variable $d_{ex}^{m_p,p}(t+\delta t)$ includes excess water generated during the vertical water balance that could not be transferred horizontally after horizontal redistribution. Cumulative water balance error for each soil material is estimated using Equation 3.13.9.

$$\hat{e}_{m_p}^p(t+\delta t) = \left| \frac{S_{m_p}^p(t+\delta t) - \hat{S}_{m_p}^p(t+\delta t)}{S_{m_p}^p(t+\delta t)} \right| \qquad (3.13.8)$$

$$\hat{E}_{m_p}^p(t+\delta t) = \hat{E}_{m_p}^p(t+\delta t) + \hat{e}_{m_p}^p(t+\delta t) \qquad (3.13.9)$$

$$\hat{S}_{m_p}^p(t+\delta t) = S_{m_p}^p(t) + \left\lfloor Q_{top}^{m_p,p} - Q_{bot}^{m_p,p} - E_{to}^{m_p,p} - E_{tu}^{m_p,p} - E_s^{m_p,p} + Q_{in}^{m_p,p} - Q_{out}^{m_p,p} + d_{ex}^{m_p,p} \right\rfloor_{t+\delta t} \qquad (3.13.7)$$

where:

$\hat{e}^{p}_{m_p}(t+\delta t)$ = proportional water balance error during the time step (-),

$\hat{E}^{p}_{m_p}(t+\delta t)$ = Cumulative proportional water balance error up to the end of current time step (-).

3.14 Generated Surface Runoff, Groundwater Runoff and Runoff Routing

A schematic diagram illustrating partitioning of the water balance components on three pixels along a single hillslope is shown in Figure 9. Typical range of the water balance fluxes under dryland conditions in NSW for pasture, trees and cropping are also shown.

3.14.1 Generated Surface Runoff

Overland flow and saturated horizontal sub-surface flow are transferred within the landscape using multiple flow path algorithm of Tarboton (1997) and Darcy's law. The method accounts for advective flux along the flow path that is determined by topography and accounts for travel times along these flow paths.

Generated surface runoff comprising overland flow and shallow sub-surface flow at each pixel on the stream p_s is added to get the total generated surface runoff as in Equation 3.14.1. Shallow sub-surface flow is defined as the horizontal sub-surface flow from all soil materials.

$$r_s(t+\delta t) = \sum_{p_s=1}^{P_s}\left(\sum_{m_p=1}^{M_p} Q_{hor}^{m_p,p_s}(t+\delta t) + q_o^{p_s}(t+\delta t)\right) \qquad (3.14.1)$$

where:

$r_s(t+\delta t)$ = total generated surface runoff over the time step $t + \delta t$ at all pixels p_s on the stream (m),

P_s = total number of pixels in the catchment located on the stream (-),

$Q_{hor}^{m_p,p_s}$ = horizontal sub-surface flow over the time step $t + \delta t$ received at soil material m_p at pixel p_s on the stream (m) (from Equations 3.12.4j to 3.12.4k),

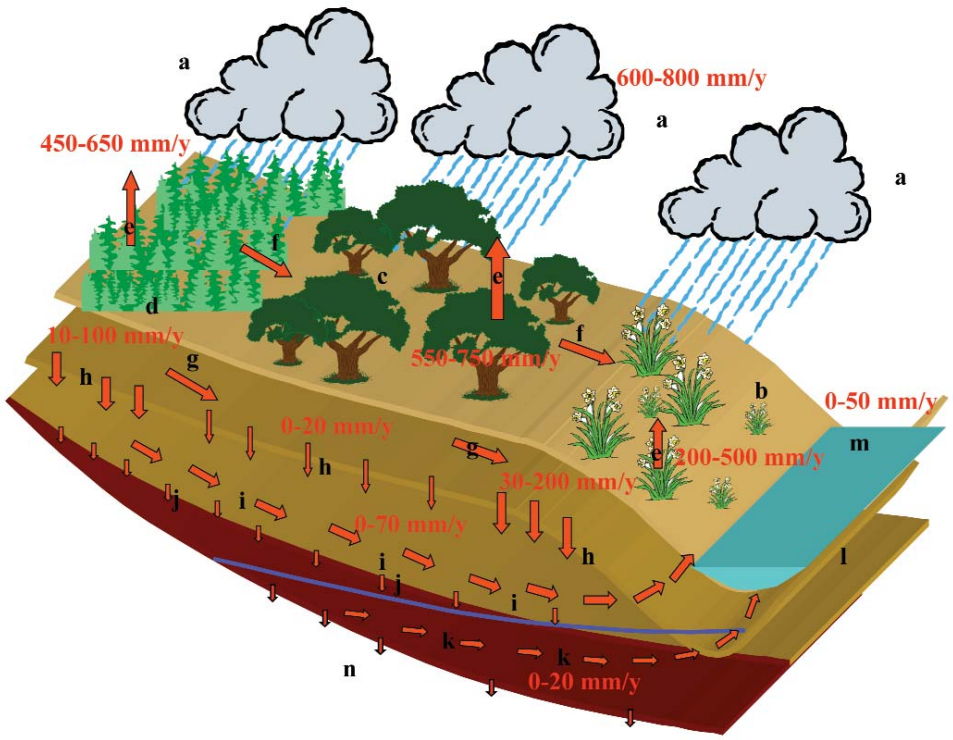

Figure 9. Schematic Diagram of Partitioning of the Water Balance Components and Simulated Landuse:- (a) rainfall, (b) crops, (c) trees, (d) pasture, (e) evapotranspiration, (f) overland flow, (g) shallow sub-surface flow, (h) drainage from the modelled soil profile, (i) lateral throughflow, (j) recharge to the Groundwater Flow System (GFS), (k) discharge from the GFS to the land (l) and to the stream (m), and (n) recharge to the regional system.

$q_o^{p_s}$ = overland flow received over the time step $t + \delta t$ at pixel p from the upslope pixels (m) (from Equation 3.11.4f).

3.14.2 Generated Groundwater Runoff and Lateral Throughflow

The catchment can be divided into a number of Groundwater Flow Systems (GFS) and such spatial data are available on a widespread basis in Australia. Metadata associated with each GFS contains the hydrogeological information ie. conductivity, transmissivity, specific yield and depth of the aquifer etc. Therefore location of each pixel within a given GFS is known from the spatial GFS datasets.

Moisture content $\theta^{1,p}(t+\delta t)$ of the deepest soil layer takes into account drainage $Q_{bot}^{m_p=1,p}(t+\delta t)$ from the soil profile according to Equations 3.11.5a to 3.11.5b using the lower boundary condition for each pixel p within a given GFS (Figure 9: h). A proportion of this drainage reaches the groundwater flow system (GFS) (Figure 9:j) from where it leaves the catchment either as discharge to stream or land or both (Figure 9:k). The remaining proportion of the drainage that cannot enter the GFS is discharged either to the land or to the stream or both through deeper sub-soil as lateral throughflow (Figure 9:*i*). Partitioning of the deep drainage into recharge to the GFS (Equation 3.14.2) and lateral throughflow can be obtained using conductivity of the sub-soil and the GFS (Equation 3.14.3).

$$Q_{rech}^{p}(t+\delta t) = \max\left(0, Q_{bot}^{m_p=1,p}(t+\delta t)\frac{K_{GFSi}^{p}}{K_{GFSi}^{p}+K_{sub}^{p}}\right) \quad (3.14.2)$$

$$Q_{lat}^{p}(t+\delta t) = Q_{bot}^{m_p=1,p}(t+\delta t) - Q_{rech}^{p}(t+\delta t) \quad (3.14.3)$$

where:

$Q_{bot}^{m_p=1,p}$ = deep drainage from bottom of the modelled soil profile at pixel p within i^{th} groundwater flow system *GFSi* (m) (Equation 3.11.24),

Q_{rech}^{p} = recharge from pixel p to the *GFSi* (m),

Q_{lat}^{p} = lateral throughflow from pixel p over the *GFSi* (m),

K_{GFSi}^{p} = saturated hydraulic conductivity of the *GFSi* where pixel p is located ($m.s^{-1}$),

K_{sub}^{p} = saturated hydraulic conductivity of the sub-soil at pixel p ($m.s^{-1}$).

The spatial distribution of the depth of soil can be predicted using the methodology of McKenzie *et al.*,(2003) (Section 3.2.2). This information on total soil depth (H_{SD}) can be used to estimate the vertical distance between depth of soil from bottom of the modelled soil profile (Md^0) and the geology of the GFS. Using this vertical distance with the conductivity of the sub-soil, travel time along the vertical to the bottom of the soil profile can be estimated (Equation 3.14.4).

$$T_{vert}^{p} = \frac{H_{SD}^{p} - (Z^{p} - Md^{0,p})}{K_{sub}^{p}} \quad (3.14.4)$$

where:

T_{vert}^{p} = travel time at pixel p along the vertical from bottom of the modelled soil profile to top of the geology (s),

H_{SD}^{p} = depth of soil at pixel p from surface to top of the geology (m),

Z^{p} = elevation of the soil surface at pixel p wrt mean sea level (m),

$Md^{0,p}$ = elevation of the bottom of the modelled soil profile at pixel p (m),

K_{sub}^{p} = saturated hydraulic conductivity of the sub-soil at pixel p ($m.s^{-1}$).

Typically average slope length in the dryland catchments across NSW varies in the range 175-250 m. FLAG landform at every pixel location is available (Section 3.2.1). This information can be used to estimate representative length of the landform L_{FLAG}^{p} (in plan) between the pixel location within a given FLAG landform and the discharge area. Using this (horizontal) length with the hydraulic conductivity of the GFS/sub-soil, horizontal travel time from the GFS or sub-soil to the discharge area can be estimated (Equations 3.14.5a to 3.14.5b). If flow path from bottom of the modelled soil profile to the GFS is vertical and along the GFS is horizontal, then maximum travel time is sum of the vertical and

horizontal travel times. However, the resultant flow path is likely to be somewhat shorter and therefore a scaler is introduced in Equations 3.14.6a to 3.14.6b. It is pointed out that modelling of preferential flow component is not included in CLASS.

$$T^p_{GFSi} = \frac{L^p_{FLAG} - L_C}{K_{GFSi}} \qquad (3.14.5a)$$

$$T^p_{lat} = \frac{L^p_{FLAG}}{K^p_{sub}} \qquad (3.14.5b)$$

$$Tlag^p_{GFSi} = \alpha_{zx}\left(T^p_{vert} + T^p_{GFSi}\right) \qquad (3.14.6a)$$

$$Tlag^p_{lat} = \alpha_{zx}\left(T^p_{vert} + T^p_{lat}\right) \qquad (3.14.6b)$$

where:

L^p_{FLAG} = average representative slope length of the FLAG landform at pixel *p* from bottom of the discharge area (*m*),

L_C = confining upslope length from the stream where the aquifer behaves as a confined/semi-confined (*m*),

K_{GFSi} = saturated hydraulic conductivity of the *GFSi* on which pixel *p* is located ($m.s^{-1}$),

K^p_{sub} = saturated hydraulic conductivity of the sub-soil on which pixel *p* is located ($m.s^{-1}$),

T^p_{GFSi} = travel time along the horizontal within the *GFSi* on which pixel *p* is located (*s*),

T^p_{lat} = travel time along the horizontal within the sub-soil on which pixel *p* is located (*s*),

$Tlag^p_{GFSi}$ = total travel time from bottom of the modelled soil profile through the sub-soil and the GFS to the discharge area (*s*),

$Tlag^p_{lat}$ = total travel time from bottom of the modelled soil profile through the sub-soil to the discharge area (*s*),

α_{zx} = scaler representing ratio of the resultant flow path and the longest flow path (≤ 1) (-).

The confining upslope length L_C is introduced in Equation 3.14.5a because pressure signal in the confined system is assumed to be much faster than the phreatic system.

Drainage from bottom of the soil profile needs to be lagged to allow for water to reach discharge areas on the land and the stream. Lagged recharge and lateral throughflow for each pixel *p* are estimated as in Equations 3.14.7 to 3.14.8.

$$Q^p_{rech}(T'_{GFS}) = Q^p_{rech}(t + \delta t) \qquad (3.14.7)$$

$$Q^p_{lat}(T'_{lat}) = Q^p_{lat}(t + \delta t) \qquad (3.14.8)$$

where:

$T'_{GFS} = t + \delta t + Tlag^p_{GFSi}$

= time lag through the sub-soil (vertical) and the GFS (horizontal) (*s*),

$T'_{lat} = t + \delta t + Tlag^p_{lat}$

= time lag through the sub-soil (vertical) and the sub-soil overlying the GFS (horizontal) (*s*).

Total discharge and lateral throughflow can be estimated by accumulating lagged recharge from all pixels *p* within a given *GFSi* (Equations 3.14.9 to 3.14.10).

where:

Q^{GFSi}_{disch} = total discharge to the land and to the stream from a given *GFSi* (*m*),

Q^{GFSi}_{lat} = total lateral throughflow to the land and to the stream from all pixels in a given *GFSi* (*m*),

L_{GFSi} = leakage to the *GFSi* to the regional groundwater system (-) ($0 \leq L_{GFSi} \leq 1$).

Discharge from the GFS is partitioned into stream discharge and land discharge as in Equations 3.14.11 to 3.14.12.

$$Q^{GFSi}_{disch}(T'_{GFS}) = Q^{GFSi}_{disch}(T'_{GFS}) + (1 - L_{GFSi})\left(Q^p_{rech}(T'_{GFS})\right)_{p \in GFSi} \qquad \forall\ p \in GFSi \qquad (3.14.9)$$

$$Q^{GFSi}_{lat}(T'_{lat}) = Q^{GFSi}_{lat}(T'_{lat}) + \left(Q^p_{lat}(T'_{lat})\right)_{p \in GFSi} \qquad \forall\ p \in GFSi \qquad (3.14.10)$$

$$Qg_{disch}^{GFSi}(T') = (1-\alpha_L)Q_{disch}^{GFSi}(T') \quad (3.14.11)$$

$$Ql_{disch}^{GFSi}(T') = \alpha_L Q_{disch}^{GFSi}(T') \quad (3.14.12)$$

where:

$Q_{disch}^{GFSi}(T')$ = lagged discharge from *GFSi* (*m*),

$Ql_{disch}^{GFSi}(T')$ = lagged discharge from *GFSi* to the land (*m*),

$Qg_{disch}^{GFSi}(T')$ = lagged discharge from *GFSi* to the stream (*m*),

α_L = partitioning coefficient of the discharge to land ($0 \le \alpha_L \le 1$; from Equation 3.14.15) (-),

$T' = T'_{GFSi}$ = lagged time (s).

Lateral throughflow from deep sub-soil over each GFS is partitioned into stream discharge and land discharge as in Equations 3.14.13 to 3.14.14.

$$Qg_{lat}^{GFSi}(T') = (1-\alpha_L)Q_{lat}^{GFSi}(T') \quad (3.14.13)$$

$$Ql_{lat}^{GFSi}(T') = \alpha_L Q_{lat}^{GFSi}(T') \quad (3.14.14)$$

where:

$Q_{lat}^{GFSi}(T')$ = lagged lateral throughflow from *GFSi* (*m*),

$Ql_{lat}^{GFSi}(T')$ = lagged lateral throughflow from *GFSi* to the land (*m*),

$Qg_{lat}^{GFSi}(T')$ = lagged lateral throughflow from *GFSi* to the stream (*m*),

$T' = T'_{lat}$ = lagged time (*s*).

The partitioning coefficient α_L of discharge from a given *GFSi* to the land is obtained as in Equation 3.14.15.

$$\alpha_L = \frac{A_L \omega_L}{A_L \omega_L + A_S \omega_S} \quad (3.14.15)$$

where:

A_L = land area in the catchment affected by shallow water table (obtained from mapped discharge areas on land and the FLAG model) (m^2),

$A_S = A_p P_s a_s$

= area of stream in the complete catchment (m^2),

A_p = area of the pixel (m^2),

P_s = total number of pixels on the stream in the catchment (-),

a_s = average proportion of the pixel area occupied by the stream (-),

ω_L = discharge weighting to land relative to the stream (-),

ω_S = discharge weighting to stream relative to itself (equal to 1)(-).

Total generated groundwater discharge to the stream and land from all the groundwater flow systems can now be estimated as in Equations 3.14.16 to 3.14.17.

$$Qg(T') = \sum_{i=1}^{NGFS} \left(Qg_{disch}^{GFSi}(T') + Qg_{lat}^{GFSi}(T') \right) \quad (3.14.16)$$

$$Ql(T') = \sum_{i=1}^{NGFS} \left(Ql_{disch}^{GFSi}(T') + Ql_{lat}^{GFSi}(T') \right) \quad (3.14.17)$$

$Qg(T')$ = total groundwater discharge to the stream (*m*),

$Ql(T')$ = total groundwater discharge to the land (*m*),

NGFS = total number of groundwater flow systems in the catchment (-).

Average upward flux for each pixel p in the discharge area on the land is estimated as Equation 3.14.18.

$$Q_v^{bot,p}(T') = \frac{Ql(T')}{P_{disch}\delta t} \quad (3.14.18)$$

where:

P_{disch} = number of pixels in discharge areas in the catchment (-),

$Q_v^{bot,p}(T')$ = average upward flux from bottom of the modelled soil profile of pixels in the discharge areas at time T' ($m.s^{-1}$),

δt = time interval of the horizontal re-distribution (s).

3.14.3 Surface Runoff Routing

Generated surface runoff component includes shallow subsurface and the overland flow components and accounts for travel time along the hillslope. Generated surface runoff (r_s) and the routed surface runoff (Q_s) represent time-averaged values over the time step $t + \delta t$. Surface runoff generated at all the pixels on the stream (from Equation 3.14.1) is routed along the stream (attenuation and lag) to the catchment outlet using the linear cascade model of Nash (1960) as in Kachroo and Liang (1992). Nash model is based on the assumption that storage in the system varies linearly with discharge from the system. Using this assumption with the differential equation describing classical mass balance, Nash (1960) obtained the general solution relating a given input of unit volume to a given output as in Equation 3.14.2.

$$h(t+\delta t) = \frac{1}{\delta t}\int_{t}^{t+\delta t} \frac{1}{K\,\Gamma(n)} \exp\left(\frac{-\tau}{K}\right)\left(\frac{\tau}{K}\right)^{n-1} d\tau \qquad (3.14.19a)$$

$$\Gamma(n) = \int_{0}^{\infty} \exp(-\tau)\tau^{n-1} d\tau \qquad (3.14.19b)$$

where:

δt = simulation time interval (s),

τ = time (s),

$K_1 = K_2 = \ldots\ldots = K_n = K$ are the storage coefficients of n linear reservoirs in cascade (units of δt),

$h(t + \delta t)$ = ordinates of the pulse response function (units of δt^{-1}) and $\Gamma(n)$ incomplete Gamma function (*dimensionless*).

It was shown by Nash (1960), that under constraints of conservation, stability, high damping and the absence of feedback, this two-parameter equation with n an integer and K positive, is almost as general a model as the differential equation of unlimited order. With additional flexibility obtained by allowing n to take fractional values, the impulse response of this equation has the ability to represent, adequately, almost all shapes commonly encountered in the hydrological context.

The assumption of linearity is largely valid and the approach works reasonably well for time scale in hours or days. However non-linear effects are pronounced when time scale and stream length is small, and the technique is less effective in describing the input-output relationship.

The linear model described by Equation 3.14.19 is the simplest representation of a causal, time-invariant, relationship between an input function of time (generated surface runoff) and the corresponding output function (routed surface runoff). It is used as a component representing the routing or diffusion effects of the catchment on those components of the generated streamflow contributing to the catchment outflow (Equation 3.14.20).

$$Q_s(t+\delta t) = \sum_{j=1}^{m'} h(j\delta t)\, r_s\left(t + \delta t - (j-1)\delta t\right) \qquad (3.14.20)$$

where:

m' = memory of the pulse response function (units of δt).

The parameter pair n and nK are chosen for optimisation, rather than n and K separately, because n is a 'shape' parameter and nK is the 'scale' parameter. Expressed in this way, the two parameters are likely to be more independent than n and K would be separately, both of which contribute to the scale and to the shape, although in different ways.

3.14.4 Groundwater Routing

Total generated groundwater discharge from landscape to the stream $Qg(T')$ is routed using similar approach as the surface runoff (Equations 3.14.19 to 3.14.20) but with separate parameters n_g and n_gK_g.

4. CLASS Solute Balance Components

A solute balance is conducted for each soil material at each pixel following water balance computations on each day.

4.1 Determining Discharge Areas in a Catchment

Water logged areas in a catchment can be determined using either mapped areas with shallow water table or from the Fuzzy Landscape Analysis GIS FLAG model (Roberts *et al.*, 1997) or both. Salt outbreak maps for large areas in New South Wales (NSW) are available. Also the outputs of the FLAG model are available for the whole state (Summerell *et al.*, 2003a,b). In the case of salinity, these maps are used in conjunction with the geology maps as a basis for describing initial salinity conditions across the catchment (Murphy *et al.*, 2003).

Fuzzy Landscape Analysis GIS (FLAG) uses gridded elevation data to calculate the wetness of soils. This model categorises grid cells based on their position in the landscape. These categories are then used to infer the landscape processes associated with their wetness and location.

FLAG uses three measures – WET-REGION, WET-LOCAL and WET-LU to derive soil wetness. For this application modelling was done at the catchment scale of 600-3000 km^2. WET-REGION is the relative height of each cell overall in the landscape, which is an indirect measure of the amount of surface and sub-surface water accumulation. As WET-REGION increases the volume of water entering a cell increases. WET-LOCAL is a measure of local lowness for a predefined area around each cell. As WET-LOCAL increases, low areas where water tables are likely to be nearer the surface are highlighted. The overall wetness indicator which uses both WET-REGION and WET-LOCAL is called WET-LU.

Combining the spatial indicator values within a GIS framework enables maps of wetness hazard to be drawn at scale of paddocks, catchments and basins. The FLAG approach thus derives scaled indicators as relative measures, and can be considered as the first iteration to guide or complement more detailed studies of changes to the water cycle, including salinisation and water logging.

4.2 Current In-stream Solute Export Model

Solute concentration time series is required as a base data set to calibrate the solute transported from landscape to the stream. In the case of salts, stream salinity measurements for catchments in NSW started on a large scale in early 1970s. Few of the sites contain continuous measured data while most sites have monthly or fortnightly measurements. For catchments where continuous salinity data are available, these can be used for calibrating salt output from the catchments. However, there are many catchments in NSW where long-term salt export rates are required but the available salinity data are either for a short period or are patchy. In such instances, a daily salt load time series can be created using an objective methodology based on stochastic hydrology concepts (Beale *et al.*, 2000; Tuteja *et al.*, 2000).

4.3 Solute Mass Balance over the Soil Material

Miscible displacement of solutes across the landscape involves three transport mechanisms, namely, advection, molecular diffusion and hydrodynamic dispersion. Dispersive and diffusive solute fluxes (hydrodynamic dispersion) that result in solute spreading in horizontal directions are neglected in the current version. Solute spreading in CLASS occurs from spreading of water down the hillslope which in turn results from multiple flow directions (Tarboton, 1997). Solute transfer between a pixel and its neighbours occurs with the respective soil materials.

Solute balance equations are written for each soil material at pixel p in the liquid and the solid phase as in Equations 4.3.1 and 4.3.2 respectively.

$$W_{m_p}^{p}(t+\delta t) = \left(W_{top}^{m_p,p} - W_{bot}^{m_p,p} - W_{to}^{m_p,p} - W_{tu}^{m_p,p} - W_{s}^{m_p,p} + SW_{in}^{m_p,p} - SW_{out}^{m_p,p} + W_{sol}^{m_p,p}\right)_{t+\delta t} + (1-\lambda_r \delta t) W_{m_p}^{p}(t) \qquad (4.3.1)$$

where:

$W_{m_p}^{p}$ = solute mass at p and soil material m_p (kg),

$W_{top}^{m_p,p}$ = solute mass at p entering from top of the soil material m_p (kg),

$W_{bot}^{m_p,p}$ = solute mass at p leaving from bottom of the soil material (kg),

$W_{to}^{m_p,p}, W_{tu}^{m_p,p}$ and $W_{s}^{m_p,p}$ = solute mass at p precipitated from the overstory and understory transpiration and the soil evaporation processes respectively (kg),

$SW_{in}^{m_p,p}$ and $(SW_{out}^{m_p,p})$ = solute mass entering (leaving) the soil material m_p at p horizontally from upslope (to downslope) pixels (kg),

$W_{sol}^{m_p,p}$ = solute mass dissolved from the soil material m_p at p (dissolved and adsorbed solutes are considered in equilibrium) (kg),

λ_r = first order rate of decay (s^{-1}),

$SS_{m_p}^{p}$ = solute concentration adsorbed to the soil (kg).

The solute mass terms $W_{to}^{m_p,p}, W_{tu}^{m_p,p}, W_{s}^{m_p,p}$ $W_{top}^{m_p,p}$, and $W_{bot}^{m_p,p}$ are obtained by multiplying the water flux terms in Equations 3.11.24 to 3.11.25 and Equations 3.13.1 to 3.13.6 with the respective solute concentration and area of the pixel. Denoting concentration of the solute in liquid and solid phase as C_w ($kg.m^{-3}$) and C_s ($g.kg^{-1}$) respectively, these terms are expressed as in Equations 4.3.3 to 4.3.6.

$$W_{tj}^{m_p,p}(t+\delta t) = A_p E_{tj}^{m_p,p}(t+\delta t) C_w^{m_p,p}(t) \quad (4.3.3)$$

$$W_{s}^{m_p,p}(t+\delta t) = A_p E_{s}^{m_p,p}(t+\delta t) C_w^{m_p,p}(t) \quad (4.3.4)$$

$$C_w^{top}(t) = \begin{cases} C_w^{m_p+1,p}(t) & \text{if } q_v^{ML(m_p)+1/2} < 0 \\ C_w^{m_p,p}(t) & \text{if } q_v^{ML(m_p)+1/2} \geq 0 \end{cases} \quad (4.3.5b)$$

$$C_w^{bot}(t) = \begin{cases} C_w^{m_p,p}(t) & \text{if } q_v^{ML(m_p-1)+1/2} < 0 \\ C_w^{m_p-1,p}(t) & \text{if } q_v^{ML(m_p-1)+1/2} \geq 0 \end{cases} \quad (4.3.6b)$$

where:

A = area of the pixel (m^2),

C_w^{GFSi} = solute concentration of the *GFSi* where pixel p is located ($kg.m^{-3}$).

The condition $q_v^{bot}(t) > 0$ can occur only if pixel p is located in the discharge area. The horizontal solute outflow from the soil material m_p is estimated using Equations 4.3.7 to 4.3.8. If solute transport is simulated, this step *must* be performed when Equations 3.12.4j to 3.12.4k are computed (see Equation 4.3.7 and Equation 4.3.8).

$$SS_{m_p}^{p}(t+\delta t) = SS_{m_p}^{p}(t) + \left(W_{to}^{m_p,p} + W_{tu}^{m_p,p} + W_{s}^{m_p,p} - W_{sol}^{m_p,p}\right)_{t+\delta t} \quad (4.3.2)$$

$$W_{top}^{m_p,p}(t+\delta t) = \begin{cases} A_p q_v^{top}(t+\delta t)\delta t C_w^{rain}(t) & \text{if } m_p = M_p \\ A_p q_v^{ML(m_p)+1/2}(t+\delta t)\delta t C_w^{top}(t) & \text{if } m_p < M_p \end{cases} \quad (4.3.5a)$$

$$W_{bot}^{m_p,p}(t+\delta t) = \begin{cases} A_p q_v^{bot}(t+\delta t)\delta t C_w^{GFSi}(t) & \text{if } m_p = 1, q_v^{bot}(t) > 0 \\ A_p q_v^{ML(m_p-1)+1/2}(t+\delta t)\delta t C_w^{bot}(t) & \text{if } 1 \leq m_p \leq M_p \end{cases} \quad (4.3.6a)$$

$$SW_{in}^{m_k,k}(t+\delta t) = SW_{in}^{m_k,k}(t+\delta t) + A_p d_{hor}^{m_p,pk}(t+\delta t) C_w^{m_p,p}(t) \quad (4.3.7)$$

$$SW_{out}^{m_p,p}(t+\delta t) = SW_{out}^{m_p,p}(t+\delta t) + A_p d_{hor}^{m_p,pk}(t+\delta t) C_w^{m_p,p}(t) \quad (4.3.8)$$

where:

$d_{hor}^{m_p,pk}$ = saturated sub-surface flow from the soil material m_p at pixel p to a neighbouring downslope pixel k (m) (from Equations 3.12.4j to 3.12.4k). The relationship between m_p and m_k is described by Equation 3.12.4a.

The Freundlich isotherm describing equilibrium exchange between dissolved and adsorbed solute concentration can be used as in Equation 4.3.9.

$$C_s = K_F (C_w)^{\alpha_F} \qquad (4.3.9)$$

where:

K_F and α_F are the parameters.

Solute mass dissolved from the soil material m_p at p (solute desorbed under equilibrium exchange) $W_{sol}^{m_p,p}$ can be estimated using Equation 4.3.10.

where:

$\hat{S}_{m_p}^{p}$ = soil moisture in the soil material m_p at p (m) (from Equation 3.13.8 at previous time step),

$P_{sat}^{m_p,p}$ = proportion soil material saturation or the specific saturation (*dimensionless*) (from Equation 3.13.6b). Specific saturation is included in Equation 4.3.10 because dissolution occurs through moisture and matrix contact surface.

Solute concentration in liquid and solid phase can be estimated as in Equations 4.3.11 and 4.3.12 respectively.

$$C_w^{m_p,p}(t+\delta t) = \frac{W_{m_p}^{p}(t+\delta t)}{A_p S_{m_p}^{p}(t+\delta t)} \qquad (4.3.11)$$

$$C_s^{m_p,p}(t+\delta t) = \frac{1000 \times SS_{m_p}^{p}(t+\delta t)}{\left(Md(m_p) - Md(m_p - 1)\right) A_p \rho_s^{m_p,p}} \qquad (4.3.12)$$

$$W_{sol}^{m_p,p}(t+\delta t) = \left(\frac{C_s^{m_p,p}(t)}{K_F}\right)^{1/\alpha_F} A \hat{S}_{m_p}^{p}(t+\delta t) P_{sat}^{m_p,p}(t+\delta t) \qquad (4.3.10)$$

where:

$C_w^{m_p,p}$ = solute concentration in liquid phase ($kg.m^{-3}$),

$C_s^{m_p,p}$ = solute concentration in solid phase ($g.kg^{-1}$),

$\rho_s^{m_p,p}$ = bulk density of the soil material m_p at p ($kg.m^{-3}$).

4.4 Solute Transport in the Stream

Surface runoff includes shallow subsurface and the overland flow components. All the solute reaching the pixel p_s defined as a stream node is pooled together as generated solute mass. The solute reaching the stream node with the lateral throughflow is also added to the stream (Equation 4.3.7). Recharge to the groundwater system is pooled separately for the GFS and the respective solute concentration is used to estimate the solute flux into the stream with groundwater discharge.

The generated solute mass is routed to the catchment outlet with the routed runoff and the assumption of fully mixed flow.

5. Time Stepping

User specified time steps are used for vertical and horizontal flux computations. Vertical flux computations for solution of the Richard's equation can be obtained at a sub-daily time step and all horizontal transfers are performed at a larger time step. It is assumed that the time step for horizontal transfers would be an integer multiple of the shorter time step used for vertical flux computations. All pasture and crop growth simulations are performed at a daily time step while all tree growth computations are performed at a monthly time step.

6. Data Requirements and Model Parameters

Data requirements for CLASS are described in this section. Parameters required by the CLASS Hydrology models U3M-1D (Vaze *et al.*, 2004), U3M-2D (Tuteja *et al.*, in prep.a) and CLASS Catchment Model (Tuteja *et al.*, in prep.c) are described in the respective User's Manual. Likewise, respective User's Manual of the models CLASS PGM, CGM and 3PG+ describe the parameters required for plant growth modelling (Vaze *et al.*, 2004a, Vaze *et al.*, 2004b; Tuteja *et al.*, in prep.b). Parameters required for spatial data relating to soil depth are described in the CLASS Spatial Analyst User's Manual (Teng *et al.*,2004).

6.1 Spatial Data Requirements

Climate data: Maximum and minimum air temperature (ºC), rainfall (mm/d), pan evaporation (mm/d), shortwave radiation ($MJ.m^{-2}$), vapour pressure (hPa), maximum and minimum relative humidity (%). These data are available from SILO database (Jeffrey *et al.*, 2001). CLASS Spatial Analyst accepts gridded data and performs climate zoning based on user specified climate zones.

DEM: Digital elevation model of any resolution. Normally, 25 m DEMs are widely used in Australia. Depending on the catchment size, the problem size may be too large. In such instances, the CLASS Spatial Analyst can coarsen the DEM in multiples of 25m, and all spatial data required by CLASS are adjusted accordingly.

FLAG upness index: Spatial data for the FLAG upness index are available for the whole of NSW (Summerell *et al.*, 2003a). Alternatively, if these data are not available, then it can be obtained using the FLAG model (Roberts *et al.*, 1997).

MRVBF Index: Spatial data for the MRVBF Index (Gallant and Dowling, 2003). If these data are not available, then it can be obtained using the functionality available in the CRCCH TIME environment (Rahman *et al.*, 2003).

Landuse: DIPNR landuse maps for the catchment, and/or the Australian Landuse Classification System – ALCC (Barson *et al.*, 2000; Stewart *et al.*, 2001).

GFS: Spatial data for the Groundwater flow systems and the associated metadata on solute concentration, hydraulic conductivity, transmissivity, specific yield and depth of aquifer. In NSW, such data are generally held in Regional databases.

Soils: Spatial data for distribution of soils. In NSW, these data are obtained using Murphy *et al.*,(2003) methodology.

Soil salinity: Spatial data for distribution of soil salinity. In NSW, these data are obtained using Murphy *et al.*,(2003) methodology. Input EC1:5 data units are in dS/m and model converts it into grams of contaminant per kilogram of soil.

6.2 Temporal Data Requirements

CLASS can be validated both in-stream as well as on the inland landscape. In-stream data are required as a minimum calibration data set. Additionally, inland landscape data relating to hydrology and plant growth would be helpful in increasing confidence in the model predictions.

Streamflow data: Streamflow data (mm/d) time series at the catchment outlet. Additional data at gauging stations within the catchment would be helpful in the calibration exercise.

Water quality data: In-stream solute concentration data ($kg.m^{-3}$) time series at the catchment outlet. Additional data at gauging stations within the catchment would be helpful in the calibration exercise.

Soil hydrology data: Soil moisture data ($m^3.m^{-3}$) time series within the catchment.

Plant growth data: Plant growth data time series within the catchment. Growth data includes LAI, stem and root biomass, groundcover etc.

7. Summary

The theoretical framework of a new distributed water and solute transport model CLASS, currently under development is presented. The model is intended for implementation on medium to large sized catchments to investigate the effects of landuse and climate variability on catchment scale. Equations for catchment scale investigation of water and solute transport including the numerical solution and interaction of the various components are detailed. The model is designed for Australian conditions and data constraints often imposed in catchment scale investigations have been taken care of in designing various components of the model. In particular the model is adapted to spatial data and tools relating to soils, topography and groundwater flow systems commonly used in Australia.

Information on spatial distribution of soils and their hydraulic properties is one of the most difficult data required in catchment scale modelling. Terrain analysis indices from the FLAG model (Roberts *et al.*, 1997; Summerell *et al.*, 2003a-b) and MRVBF (Gallant and Dowling, 2003) are combined and used to describe various landforms along the hillslopes. These are then combined with the soil landscape mapping and the geologies using the framework of Murphy *et al.*,(2003) to predict the spatial distribution of the soil types and soil physical properties. The properties of the soil types are identified from available soil survey data and these properties are then translated into soil hydraulic properties using PTFs from Minasny and McBratney (2002). The soil salinity properties are predicted from the soil survey data.

The model includes comprehensive hydrology and growth components. The growth model includes annual and perennial pastures (C_3 and C_4) along with a legume, cropping and trees. The algorithms for the growth model are sourced from Johnson (2003).

Recharge and discharge areas are spatially defined a-priori as input using information on mapped areas of shallow water table and the FLAG model. For each pixel located in the catchment, water balance is performed in the unsaturated zone along the vertical axis using the Richard's equation. A specified flux boundary condition is used at the soil surface that includes atmospheric flux and overland flow contribution from the upslope areas. The upslope boundary condition includes horizontal sub-surface flow in each soil material from the respective soil material from all neighbouring upslope pixels. A free drainage boundary condition is used at the bottom of the modelled soil profile in the recharge areas. In the discharge areas, an upward flux boundary condition is used at the bottom with flux estimated from land discharge from upslope areas. When the land discharge to the pixel in a discharge area is zero (dry conditions), a free drainage boundary condition is used at the bottom.

The vertical water balance in the unsaturated zone is performed at a shorter time step relative to the time step for horizontal transfers. Vertical fluxes at a given pixel are accumulated over the horizontal time step. Moisture in excess of soil moisture holding capacity is transferred horizontally to the neighbouring downslope pixels. Horizontal transfers occur between the respective soil materials using the multiple flow path algorithm of Tarboton (1997) and Darcy's law. Horizontal transfers occur within the respective soil materials (eg. topsoil material of a given pixel to the topsoil material of the neighbouring downslope pixels).

Drainage from the modelled soil profile is partitioned into recharge to the underlying groundwater flow system (GFS) and lateral throughflow. Lateral throughflow comprises water that cannot enter the aquifer and is transferred horizontally within the sub-soil to either the discharge areas on the land or to the stream or both. Recharge and lateral throughflow each are pooled over the GFS. A proportion of each of these components is passed to the land as surface discharge and the remaining component is passed to the stream. Discharge to the land is lagged appropriately and then used as the upward flux boundary condition in the vertical water balance (upward flux boundary condition). This time lag is based on the assumption that the bulk of the travel time results where the flow occurs under phreatic conditions and that a fast pressure transmission signal applies in the confined system.

Generated surface runoff comprising overland flow

and shallow sub-surface flow is pooled at all pixels on the stream. Travel times along the hillslopes is accounted for in horizontal transfers. Generated surface runoff and groundwater runoff, are routed using the Nash model through separate response functions to the catchment outlet.

Solute transport in the landscape accounts for advection, but transport mechanisms associated with hydrodynamic dispersion are ignored. Solute transport in the stream includes solute sources from various pathways and is routed to the catchment outlet with water using the assumption of fully mixed flow.

8. Software Platform Related Issues

The CLASS modelling framework is developed on the Microsoft.Net platform. The spatial components are written in VB.Net and currently operational on ARCGIS8.3. Most of the aspatial model components are written in C#.Net. In 2004-05, the CLASS modelling framework will be incorporated into Toolkit Modelling Environment developed by the Cooperative Research Centre for Catchment Hydrology (Rahman *et al.*, 2003).

11. References

Abbott, M. B., J. C. Bathurst, J. A Cunge., P. E. O'Connell, J. Rasmussen. 1986. An introduction to the European hydrological system – systeme hydrologique Europeen SHE, 1. History and philosophy of a physically-based distributed modelling system. *Journal of Hydrology* **87**: 45-59.

Australian Bureau of Meteorology. 2001. Climate Atlas of Australia: Evapotranspiration. Bureau of Meteorology. ISBN 0642 320 489.

Band, L. E., P. Patterson, R. Nemani, and S. W. Running. 1993. Forest ecosystem processes at the watershed scale: Incorporating hillslope hydrology. *Agric. For. Meteorol.* **63**, 93-126.

Barson, M. M., L. A. Randall and V.L. Bordas, and Cover Change in Australia. Results of the collaborative Bureau of Rural Sciences - State agencies' Project on Remote Sensing of Land Cover Change. B*ureau of Rural Sciences*, Canberra, 2000.

Beer, T., 1990. Applied Environmetrics Meteorological Tables. Applied Environmetrics, Balwyn, Victoria, Australia, 56p.

Beven, K. J., M. J. Kirkby. 1979. A physically-based variable contributing area model of basin hydrology. *Hydrological Science Bulletin* **24**: 43-69.

Beven, K., and J. Freer. 2001. A Dynamic TOPMODEL. *Hydrological Processes* **15**, 1993-2011.

Bronstert, A. 1995.User manual for the hillflow-3D catchment modelling system. Working document 95/4, CRC for Catchment Hydrology, Australia.

Brooks, R.H., and A.T. Corey. Properties of porous media affecting fluid flow, *Journal of the Irrigation & Drainage Division 2 (June)*, American Society of Civil Engineers, pp 61-88, 1966

Burman, R., and L.O. Pochop. 1994. Evaporation, evapotranspiration and climatic data. Elsevier, Amsterdam, 278p.

Burman, R., R.H. Cuenca, and A.Weiss. 1983. Techniques for estimating irrigation water requirements. In Hillel (1983), pp. 335-394.

Carsel, R.F., and R.S. Parrish, Developing joint probability distributions of soil water retention characteristics, Water Resources Research, 24: 755-769, 1988.

Costa-Cabral, M., and S. J. Burges. 1994. Digital elevation model networks (DEMON): A model for flow over hillslope for computation of contributing and dispersal areas. *Water Resources Research* **30** (6): 1681-1692.

Dawes, W., and T. Hatton. 1993. TOPOG_IRM 1. Model description, Technical memorandum 93/5, CSIRO Division of Water Resources, Australia.

Dickinson, R.E., A. Henderson-Sellers, C. Rosenzweig, and P. J. Sellers. 1991. Evapotranspiration models with canopy resistance for use in climate models. A review, *Agric. For. Meteorol.* **54,** 373-388.

DLWC. 2000. The New South Wales Salinity Strategy – Taking on the Challenge. NSW Department of Land and Water Conservation, August 2000. ISBN 0 7347 5146 X

Dolezal, F. 2002. Report on outcomes of work, 5 March-27 June 2002, unpublished data.

Dolezal, F. 1994. Physical Processes, Unpublished lecture notes - *International Post Graduate Hydrology Course 1993-94*, University College Galway, Ireland.

Dunin, F.X., E.M. O'Loughlin, W. Reyenga, 1988. Interception loss from Eucalypt forest: Lysimeter determination of hourly rates for long term evaluation, *Hydrological Processes*, vol. 2, 315-329.

Famiglietti, J. S., E. F. Wood, M. Sivapalan, and D. J. Thongs. 1992. A catchment scale water balance model for FIFE, J. *Geophys. Res.* **97**(D17): 18,997-19,007.

Gallant, J.C., and T.I.Dowling. 2003. A multi-resolution index of valley bottom flatness for mapping depositional areas, *Water Resources Research*, vol. **39** no. 1, 1347.

Grayson, R.B. and A.W.Western. 2001. Terrain and the distribution of soil moisture, *Hydrological Processes*, 15(13): 2689-2690.

Grayson, R.B. and G.Blöschl. 2000. Spatial Patterns in Catchment Hydrology: Observations and Modelling. *Cambridge University Press*. 404p.

Holmes, J. W., J. A Sinclair. 1986. Water yield from some afforested catchments in Victoria, Paper presented at Hydrology and Water Resources Symposium, Inst. Of Eng., Brisbane, Queensland, Australia, Nov. 25-27.

Idso, S.B., 1981. A set of equations for full spectrum and 8 -14 um and 10.5 - 12.5 um thermal radiation from cloudless skies. *Water Resources Research*, **17**, 295-304.

Jeffrey, S. J., J. O. Carter, K. B. Moodie, A. R. Beswick. 2001. Using spatial interpolation to construct a comprehensive archive of Australian climate data. *Environmental Modelling and Software* **16**: 309-330.

Johnson, I.R., 2003. A mathematical approach to modelling pastures and crops for Australian conditions, A consultancy report prepared for the NSW Dept of Infrastructure Planning and Natural Resources.

Kachroo, R.K., 'River flow forecasting. Part 5. Applications of a conceptual model', *Journal of Hydrology*, 133, 141-178, 1992.

Kandel, D., A. Western, R. Grayson, H. Turral. 2002. Surface runoff modelling: Part 2. Parameterisation at process timescale using plot scale data from a mid-hill catchment of Nepal. Proceedings of the 27th Hydrology and Water Resources Symposium 2002, Hilton on the Park - Melbourne: Australia.

Landsberg, J. J., and R. H Waring. 1997. A generalised model of forest productivity using simplified concepts of radiation-use efficiency, carbon balance and partitioning. *Forest Ecology and Management* **95**(1997): 209-228.

Lea, N.L. 1992. An aspect driven kinematic routing algorithm, In Overland Flow: Hyd. and Erosion Mechanics, Ed. A.J. Parsons and A.D. Abrahams, *Chapman and Hall*, New York.

Littleboy, M., D. M. Silburn, D. M. Freebairn, D. R. Woodruff, G. L. Hammer, and J. K. Leslie. 1992. Impact of erosion on production in cropping systems. I. Development and validation of a simulation model. *Aust. J. of Soil Res*. **30**: 757-774

McCown, R.L., G. L. Hammer, J. N. G. Hargraves, D. L. Holzworth, and D. M. Freebairn. 1996. APSIM - A novel software system for model development, model testing, and simulation in agricultural systems research. *Agricultural systems* **50**: 255-271.

McDonald, R. C., R. F. Isbell, J. G. Speight, J. Walker, M. S. Hopkins. 1990. Australian Soil and Land Survey Field Handbook, 2nd ed. *Inkata Press*: Melbourne.

McKenzie, N.J., J.C. Gallant, and L.J. Gregory, 2003. Estimating Water Storage Capacities in Soil at Catchment Scales. Technical Report 03/3, Cooperative Research Centre for Catchment Hydrology, Australia.

MDBMC. 2001. Basin Salinity Management Strategy 2001 – 2015. Murray-Darling Basin Ministerial Council. Ref. No I&D 6719. August 2001. ISBN 1 876830 17 4. (http://www.mdbc.gov.au).

Minasny, B., and A. B. McBratney. 2002. The neuro-m method for fitting neural network parametric pedotransfer functions. *Soil Sci. Soc. Am. J.* **66**: 352-361.

Monteith, J. L. 1973. Principles of Environmental Physics, American Elsevier, New York.

Monteith, J. L. 1981. Evaporation and surface temperature, *Q. J. R. Meteorol. Soc.* **107**: 1-27.

Monteith, J.L., and M.H.Unsworth, 1990. Principles of Environmental Physics, Second Edition, E. Arnold, London.

Morris, J., 2003. Predicting the environmental interactions of Eucalyptus plantations using a process-based forest model. International Symposium on Eucalypts in Asia (ISEA). Zhanjiang, China, April 2003. ACIAR Publications, Canberra (in press).

Murphy, B., G. Geeves., M. Miller, G. Summerell, P. Southwell, and M. Rankin. 2003. The Application of Pedotransfer Functions with Existing Soil Maps to Predict Soil Hydraulic Properties for Catchment – Scale Hydrologic and Salinity Modelling, MODSIM 2003, International Conference held at Townsville, Australia, July 2003.

Nash, J. E. 1960. A unit hydrograph study with particular reference to British catchments. Proc. Inst. Civ. Eng. 17: 249-282.

Nash, J. E., and J. Sutcliffe. 1970. River flow forecasting through conceptual models, Part 1, A discussion of principles. *Journal of Hydrology* **10**: 282-290.

O'Callaghan, J.F., and D. M. Mark. 1984. The extraction of drainage networks from digital elevation data. *Computer Vision, Graphics and Image Processing* **28**:328-344.

Quinn, P., K. Beven, P. Chevallier, and Planchon. 1991, The prediction of hillslope flow paths for distributed hydrological modelling using digital terrain models. *Hydrological Processes* **5**: 59-80.

Rahman, J.M., S.P. Seaton, J-M. Perraud, H. Hotham, D.I. Verrelli, and J.R. Coleman, 2003. It's TIME for a New Environmental Modelling Framework, in proceedings of MODSIM 2003, 1727-1732

Richard, L. A. 1931. Capillary conduction of liquids through porous mediums. *Physics* **1**: 318-333.

Ringrose-Voase A, and H. Cresswell. 2000. Measurement and prediction of deep drainage under current and alternative farming practice. Final Report to the Land and Water Resources Research and Development Corporation Project CDS16, CSIRO Land and Water, Australia.

Roberts, D. W., T. I. Dowling, and J. Walker. 1997. FLAG: A Fuzzy Landscape Analysis GIS Method for Dryland Salinity Assessment, CSIRO Land and Water, Technical Report No 8/97.

Ruprecht, J. K., M. Sivapalan. 1991. Salinity modelling of experimental catchments. *Proceedings of International Hydrology and Water Resources Symposium*, Perth. Australia 2-4 October.

Schaap, M.G., and J. Leij. 1998. Database-related accuracy and uncertainty of pedotransfer functions, *Soil Science*, vol.163, **10**:765-779.

Sharpley, A.N., J.R. Williams, 1990. EPIC – Erosion/Productivity Impact Calculator: 1. Model documentation, 2. User's guide, USDA Technical Bulleting No. 1768, 1990.

Shuttleworth, W. J., and J. S. Wallace. 1985. Evaporation from sparse crops—An energy combination theory, *Q. J. R. Meteorol. Soc.* **111**: 839-855.

Sivapalan, M., K. Beven, and E. F. Wood. 1987. On hydrologic similarity, 2, A scaled model of storm runoff production, *Water Resources Research* **23**(12), 2266-2278.

Smith, M., 1991. Report on expert consultation on procedures for revision of FAO guidelines for prediction of crop water requirements (Rome, Italy, 28-31 May, 1990). FAO Land and Water Development Division, Rome, 54pp.

Stace, H. C. T., G. D. Hubble, R. Brewer, K. H. Northcote, J. R. Sleeman, M. J. Mulcahy, and E. G. Hallsworth. 1968. A Handbook of Australian Soils. *Rellim Technical Publications*, Glenside, South Australia.

Stewart, J.B., Smart, R.V., Barry, S.C. and Veitch, S.M., 1996/97 Land Use of Australia - Final Report for Project BRR5 , *National Land and Water Resources Audit*, Canberra, 2001.

Summerell, G. K., G. B. Beale, M. L. Miller and T. I. Dowling. 2003a. DLWC-FLAG modelling of soil wetness hazard in upland NSW: A user manual to access and interpret soil wetness maps. NSW Department of Land and Water Conservation, Centre for Natural Resources, Sydney. **Y03-614**

Summerell, G.K., J. Vaze, N.K. Tuteja, R.B. Grayson, and T.I. Dowling, 2003b. Development of an objective terrain analysis based method for delineating the major landforms of catchments. *MODSIM 2003*, International Conference held at Townsville, Australia, July 2003.

Tarboton, D. G. 1997. A new method for the determination of flow directions and upslope areas in grid digital elevation models. *Water Resources Research* **33**: 309-319.

Teng, J., J. Vaze and N.K. Tuteja, 2004. CLASS Spatial Analyst. User's Manual (ISBN 0 7347 5516 3). NSW Department of Infrastructure, Planning and Natural Resources, Australia and Cooperative Research Centre for Catchment Hydrology, Australia.

Thom, A. S. 1972. Momentum, mass and heat exchange of vegetation, Q*uart. J. R. Met. Soc.* **198**: 124-134.

Thornley, J.H.M. and I.R. Johnson, 2000. Plant and Crop Modelling: *A mathematical approach to plant and crop physiology*, The Blackburn Press, ISBN 1930665059.

Turner, K. M. 1991. Annual evapotranspiration of native vegetation in a Mediterranean-type climate. *Water Resource Bulletin* **27**: 1-6.

Tuteja, N. K., J. Vaze, G. T. H. Beale, G. Summerell, M. Miller. 2003. Spatial disaggregation of the catchment scale fluxes. *MODSIM 2003*, International Conference held at Townsville, Australia, July 2003.

Tuteja, N.K., G. Beale, W. Dawes,J. Vaze, B. Murphy, P. Barnett, A. Rancic, R. Evans, G. Geeves, D.W. Rassam, and M. Miller, 2003. Predicting the effects of landuse change on water and salt balance – a case study of a catchment affected by dryland salinity in NSW, Australia, *Journal of Hydrology*, vol **283**/1-4, 67-90.

Tuteja, N.K., G.T.H. Beale, G.K. Summerell, and W.H. Johnston, 2002. Development and validation of the catchment scale salt balance model CATSALT version 1. *NSW Department of Land and Water Conservation*, CNR 2001.031, ISBN 0 7347 5244 X.

Tuteja, N.K., J. Teng, and J.Vaze. (in prep.a). CLASS 2-Dimensional Unsaturated Moisture Movement Mode U3M-2D. User's Manual. NSW Department of Infrastructure, Planning and Natural Resources, Australia and Cooperative Research Centre for Catchment Hydrology, Australia.

Tuteja, N.K., J. Teng, J. Vaze, and J.M. Morris, (in prep.b). CLASS 3PG+ Tree Growth Model. User's Manual. NSW Department of Infrastructure, Planning and Natural Resources, Australia and Cooperative Research Centre for Catchment Hydrology, Australia.

Tuteja, N.K., J. Vaze, J. Teng, B.W. Murphy, and G.Beale (in prep.c). CLASS Catchment Model. User's Manual. NSW Department of Infrastructure, Planning and Natural Resources, Australia and Cooperative Research Centre for Catchment Hydrology, Australia.

van Bavel, C. H. M., and D. Hillel. 1976. Calculating potential and actual evaporation from a bare soil surface by simulation of concurrent flow of water and heat. *Agr. Meteorol.* **17**: 453-476.

van Genuchten M. Th. 1980, A Closed Form Equation for Predicting the Hydraulic Conductivity of Unsaturated Soils, *Soil Sc. Soc. Am. J.*, 48, 703-708.

Vaze, J., G. T. H. Beale, P. Barnett, N. K. Tuteja. 2003. Predicting the spatial and temporal effects of landuse change using the CATSALT modelling framework. *MODSIM 2003*, International Conference held at Townsville, Australia, July 2003.

Vaze, J., P. Barnett, G. T. H. Beale, W. Dawes, R. Evans, N. K. Tuteja, B. Murphy, G. Geeves, and M. Miller. 2004. Modelling the effects of landuse change on water and salt delivery from a catchment affected by dryland salinity in south-east Australia, *Hydrological Processes*, **18**, 1613-1637.

Vaze, J., J.Teng, N.K. Tuteja (2004a). CLASS PGM – Pasture Growth Model. User's Manual (ISBN 0 7347 5514 7) NSW Department of Infrastructure, Planning and Natural Resources, Australia and Cooperative Research Centre for Catchment Hydrology, Australia.

Vaze, J., J. Teng, N.K. Tuteja, (2004b). CLASS CGM – Crop Growth Model. User's Manual (ISBN 0 7347 5515 5). NSW Department of Infrastructure, Planning and Natural Resources, Australia and Cooperative Research Centre for Catchment Hydrology, Australia.

Vaze, J., N.K. Tuteja, J. Teng, 2004. CLASS Unsaturated Moisture Movement Model U3M-1D. User's Manual (ISBN 0 7347 5513 9). NSW Department of Infrastructure, Planning and Natural Resources, Australia and Cooperative Research Centre for Catchment Hydrology, Australia.

Vertessy, R. A., T. J. Hatton, R. G. Benyon, W. R. J. Dawes. 1996. Long term growth and water balance for a mountain ash (Eucalyptus Regnans) forest catchment subject to clear felling and regeneration. *Tree Physiology* **16**: 221-232.

Vogel, T., and M. Cislerová, On the Reliability of Unsaturated Hydraulic Conductivity Calculated from the Moisture Retention Curve, *Transport in Porous Media*, **3**, 1-15, 1988.

Walker, J., F. Bullen, J. Williams. 1992. Hydroecological changes in the Murray Darling Basin. 1: The number of trees cleared over two centuries. *Journal of Applied Ecology* **30**: 265-273

Watson, F. G. R., R. A. Vertessy, R. B. Grayson. 1999. Large-scale modelling of forest hydrological processes and their long-term effect on water yield. *Hydrological Processes* **13**: 689-700.

Watson, F.G.R., R.B. Grayson, R.A.Vertessy, M.C. Peel, and L.L.Pierce. 2001. Evolution of a hillslope hydrological model. International Conference on Modelling and Simulation *MODSIM 2001*, Canberra, Australia, 10-13 December 2001. 461-467.

Wigmosta, M. S., and D. P. Lettenmaier. 1999. A comparison of simplified methods for routing topographically driven subsurface flow. *Water Resources Research*, *Vol. 35*, **1**: 255-264.

Wigmosta, M. S., L. W. Vail, D. P. Lettenmaier. 1994. A distributed hydrology-vegetation model for complex terrain. *Water resources research, Vol. 30,***6**: 1665-1679.

Williamson, D., G. Gates, G. Robinson, G. Linke, M. Seker, W. Evans. 1997. Salt trends: Historic trend in salt concentration and saltload of stream flow in the Murray-Darling drainage basin. Dryland technical report No. 1, Murray-Darling Basin Commission.

Wösten, J. H. M., P. A. Finke, and M. J. W. Jansen. 1995. Comparison of class and continuous pedotransfer functions to generate soil hydraulic characteristics. *Geoderma* **66**:227-237.

Yu, B., C. Rose, K. Coughlan, B. Fentie. 1997. Plot-scale rainfall-runoff characteristics and modelling at six sites in Australia and Southeast Asia. *Transactions of the ASAE* **40**(5): 1295-1303.

Zhang, L., W. R. Dawes, G. R. Walker. 2001. Response of mean annual evapotranspiration to vegetation changes at a catchment scale. *Water Resources Research* **37**: 701-708

CENTRE OFFICE

CRC for Catchment Hydrology
Department of Civil Engineering
Building 60
Monash University
Victoria 3800
Australia

Tel +61 3 9905 2704
Fax +61 3 9905 5033
email crcch@eng.monash.edu.au
www.catchment.crc.org.au

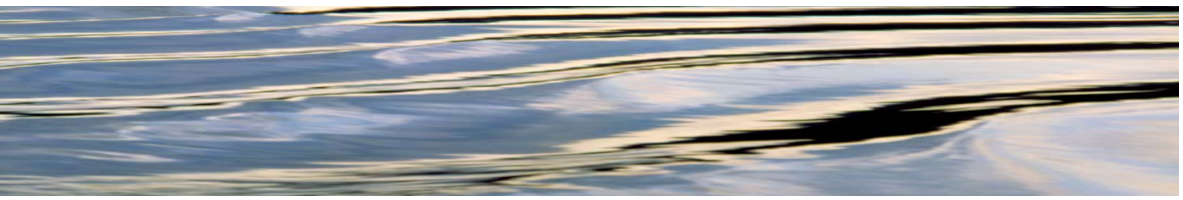

The Cooperative Research Centre for Catchment Hydrology is a cooperative venture formed under the Australian Government's CRC Programme between:

- Brisbane City Council
- Bureau of Meteorology
- CSIRO Land and Water
- Department of Infrastructure, Planning and Natural Resources, NSW
- Department of Sustainability and Environment, Vic
- Goulburn-Murray Water
- Grampians Wimmera Mallee Water
- Griffith University
- Melbourne Water
- Monash University
- Murray-Darling Basin Commission
- Natural Resources, Mines and Energy, Qld
- Southern Rural Water
- The University of Melbourne

ASSOCIATE:

- Water Corporation of Western Australia

RESEARCH AFFILIATES:

- Australian National University
- National Institute of Water and Atmospheric Research, New Zealand
- Sustainable Water Resources Research Center, Republic of Korea
- University of New South Wales

INDUSTRY AFFILIATES:

- Earth Tech
- Ecological Engineering
- Sinclair Knight Merz
- WBM

CRC AUSTRALIA

Established and supported under the Australian Government's Cooperative Research Centre Program

COOPERATIVE RESEARCH CENTRE FOR
CATCHMENT HYDROLOGY